Multidimensional Resilience Decision-Making for Complex and Substructured Systems

Julian Salomon[a,*], Jasper Behrensdorf[a], Niklas Winnewisser[a], Matteo Broggi[a], Michael Beer[a,b,c]

[a] *Institute for Risk and Reliability, Leibniz University Hannover, Hanover, Germany.*
[b] *Institute for Risk and Uncertainty, University of Liverpool, Liverpool, United Kingdom.*
[c] *International Joint Research Center for Resilient Infrastructure & International Joint Research Center for Engineering Reliability and Stochastic Mechanics, Tongji University, Shanghai, China.*

Abstract

Complex systems, such as infrastructure networks, industrial plants and jet engines, are of paramount importance to modern societies. However, these systems are subject to a variety of different threats. Novel research focuses not only on monitoring and improving the robustness and reliability of systems, but also on their recoverability from adverse events. The concept of resilience encompasses precisely these aspects. However, efficient resilience analysis for the modern systems of our societies is becoming more and more challenging. Due to their increasing complexity, system components frequently exhibit significant complexity of their own, requiring them to be modeled as systems, i.e., subsystems. Therefore, efficient resilience analysis approaches are needed to address this emerging challenge.

This work presents an efficient resilience decision-making procedure for complex and substructured systems. A novel methodology is derived by bringing together two methods from the fields of reliability analysis and modern resilience assessment. A resilience decision-making framework and the concept of survival signature are extended and merged, providing an efficient approach for quantifying the resilience of complex, large and substructured systems subject to monetary restrictions. The new approach combines both of the advantageous characteristics of its two original components: A direct comparison between various resilience-enhancing options from a multidimensional search space, leading to an optimal trade-off with respect to the system resilience and a significant reduction of the computational effort due to the separation property of the survival signature, once a subsystem structure has been computed, any possible characterization of the probabilistic part can be validated with no need to recompute the structure.

The developed methods are applied to the functional model of a multistage high-speed axial compressor and two substructured systems of increasing complexity, providing accurate results and demonstrating efficiency and general applicability.

Keywords: Resilience, Decision-Making, Survival Signature, Reliability, Complex Systems, Substructured Systems

1. Introduction

In today's highly developed societies, complex systems, such as infrastructure networks, industrial plants and jet engines are both ubiquitous and of paramount importance to the functioning of these modern societies. It is evident that these systems are exposed to a variety of harmful influences of natural, technical and anthropogenic origin. At the same time, as Punzo et al. highlight in [1], "It is an undeniable fact that modern day systems are more integrated, more interdependent, evolve at faster pace and, in a word, are more complex than the systems of the previous century [...]". Considering this high and increasing system complexity, it is impractical to detect and prevent all potential negative impacts. Therefore, it is essential that new developments in engineering focus not only on monitoring and improving the robustness and reliability of systems, but also on their recoverability after adverse events [2]. The concept of resilience encompasses these aspects: analyzing and optimizing robustness, reliability and recovery of systems, from a technical and economic perspective [3, 4, 5]. Applying resilience to engineered systems leads to a paradigm shift. Secure systems cannot solely rely on strategies to prevent failures, but must include strategies for efficient recovery in the event of failure as well, see, e.g., [6, 7].

In engineering, the concept of resilience has steadily gained popularity in recent years [8, 9, 1]. The notion of "resilience" appears in various fields such as ecology, economics, and psychology, as well as in the context of mechanical systems, and is derived from the Latin word "resilire," which means "to bounce back." The concept of resilience was first introduced by Holling in the field of ecological systems [10]. Although several other definitions by various scientists followed, most of them have certain key aspects in common that were already captured by Holling's early definition [11, 12, 13, 14, 15]. In [16], Ayyub provides a literature review and develops a comprehensive definition of resilience in the context of complex systems based on the content of the Presidential Policy Directive (PPD) on critical infrastructure security and resilience [17]. His definition provides a solid foundation for quantifying resilience.

Numerous options exist for improving the resilience of complex systems. However, resources are not unlimited and re-

*Corresponding author
Email address: salomon@irz.uni-hannover.de (Julian Salomon)

silience cannot be increased at will. Therefore, it is essential not only to be able to distinguish and weigh between a variety of different resilience-enhancing measures, but to also consider their monetary aspects [18, 19]. In [20], Salomon et al. present a method for identifying the most cost-effective allocation of resilience-enhancing investments by merging the resilience metric of [21] and an adaptation of the systemic risk measure of [22]. Their approach allows for a direct comparison of the effects of heterogeneous controls on the resilience of a system over an arbitrary time period in a two-dimensional parameter space.

Additionally, current research in the context of resilience focuses on improved resilience quantification measures, as proposed in [23], and overarching frameworks for stakeholder decision-making, e.g., for transportation networks in the presence of seismic hazards [24]. For a comprehensive literature review on resilience assessment frameworks that balance resources and performance, see [25]. Other researchers recently studied the complexity of realistic infrastructure systems, failure consequences, recovery sequences, and varying external effects. In [26], for example, the authors revealed the vast complexity of modern critical infrastructures and their multi-factorial nature as cyber-human-physical systems and studied appropriate modeling and resilience analysis approaches. Further, the works [27] and [28] are concerned with the effects on decision-making when considering stakeholder preferences or enhancement and recovery strategies. External effects and challenges arising from climate change were studied in the context of resilience, e.g., in [29].

Various technical and infrastructural systems in today's society are large and complex in nature. In particular, when system components have such complexity that they themselves need to be modeled as systems, so-called systems of systems [30, 31], resulting in a significantly high number of components. This is in accordance to Batty, who highlights "A very simple definition of a complex system is 'a system that is composed of complex systems"' [32]. As each of the subsystems affects the top-level system under consideration, this causes a significant increase in computational effort for system analysis and constitutes a major challenge [33, 34]. Therefore, it is particularly important to have tools capable of efficiently assessing all three resilience phases. Typically the reliability phase involves the most system evaluations, in particular when various different system configurations need to be assessed that have an impact on the probability structure of the subsystems and thus on the overall system. Therefore, a particularly efficient analysis approach is required for this phase.

An efficient approach to modeling the reliability of systems with multiple component types is provided by the concept of survival signature, introduced and discussed in [35, 36] by Coolen and Coolen-Maturi. Its major benefit over conventional approaches is the separation of the system structure from the probabilistic properties of the system components. Once the system structure has been analyzed, any possible probabilistic characterization can be tested without having to reevaluate any system states. Consequently, this approach reduces the computational cost of repeated model evaluations typically required in design and maintenance processes [37]. Current research is focused on multi-state components [37], common cause failures [38], multiple failure modes and dependent failures [39], approximation techniques for large systems [40] and reliability analysis in consideration of imprecision [41].

In this paper, theoretical fundamentals are summarized and the resilience decision-making method introduced in [20] is extended to multidimensional parameter spaces. Next, a novel and encompassing methodology is developed, consisting of its two major ingredients, the extended resilience decision-making method and the survival signature. This allows for an efficient and multidimensional resilience analysis of complex, large and substructured systems. The extension and novel methodology are then applied to a functional model of a multistage high-speed axial compressor, an arbitrary complex system as well as the U-Bahn and S-Bahn system of Berlin, to prove general applicability.

2. Resilience Decision-Making

Assessing the resilience of complex systems subject to technical or monetary constraints requires a sophisticated methodology to efficiently derive optimal decisions. In [20], Salomon et al. propose a versatile approach with three key elements, including a metric for resilience quantification, an adapted systemic risk measure, and a grid search algorithm that increases computational efficiency.

2.1. Resilience Quantification

A suitable quantitative measure of resilience is a fundamental prerequisite for assessing resilience in engineering. In [8, 42, 43], the authors provide a comprehensive overview of resilience metrics in a systemic context. While Bergström et al. emphasize the general concept of resilience in the current literature as a critical link between increasing complexity of systems and their risk [8], Sun et al. focus on resilience of infrastructures and highlight the close link between resilience and functionality respectively performance measures [43]. Hosseini et al. proposed a general scheme for categorizing resilience quantification approaches [42]. In summary, performance-based resilience metrics are most widely used. These determine the resilience of a system by comparing its performance before and after a destructive event. Further subcategories relate to time in-/dependence and characterization as deterministic or probabilistic processes.

According to [44] and [42], performance-based and time-dependent metrics are capable of considering the following system and transition states before and after a disruptive event:

- The original stable state, i.e., the duration until a disruptive event occurs, relying on the reliability of the system.
- The system vulnerability, represented by a loss of performance after the occurrence of a disruptive event and the robustness counteracting the vulnerability and mitigating this performance loss. Both are governed by degradation characteristics of the system components.
- The system recoverability, characterized by the disrupted state of the system and its recovery to a new stable state.

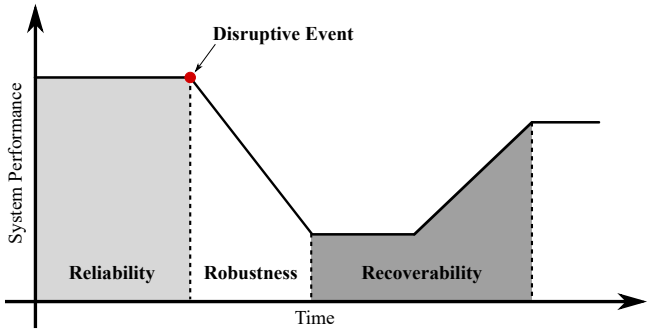

Figure 1: In the evolution of a system before and after the impact of a disruptive event, different phases can be distinguished: (i) the original stable state, (ii) disruptive impact, vulnerability, robustness, (iii) disrupted state and recovery; adapted from [44].

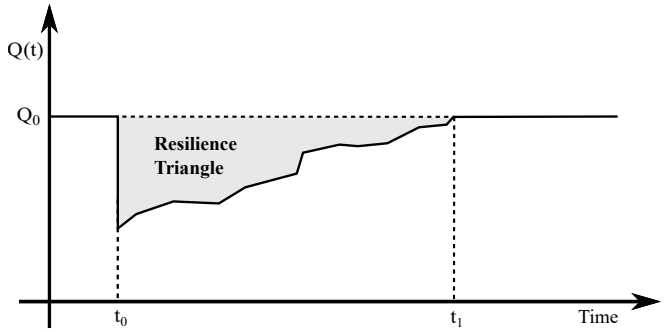

Figure 2: Resilience triangle; adapted from [45].

An illustration of these phases and transitions is shown in Fig. 1. The performance level of the new stable state might differ from the performance level of the original state.

The area of performance loss between original and new stable state in Fig. 1 refers to the well-known principle of "*resilience triangle*" introduced by Bruneau et al. [45], as illustrated in Fig. 2. In their work, Bruneau et al. proposed a time-dependent, performance-based, and deterministic metric for resilience loss of a community due to seismic disasters as follows. Let t_0 be the time a disruptive event occurs and t_1 be the time of completed recovery. Further, $Q(t)$ denotes the quality of the community infrastructure at time t, specifying the type of system performance. Then, the metric is defined as:

$$R_{Br} = \int_{t_0}^{t_1} [100 - Q(t)]dt. \tag{1}$$

Note that the system performance is compared with a time-independent ideal performance of 100 in the considered interval of performance loss. The approach forms a strong basis for several, later proposed metrics in various contexts, see [46, 47, 48].

In [20], Salomon et al. utilize the probabilistic and time-dependent metric developed by Ouyang et al. [21]. The metric is defined as the expected ratio of the integral over the actual system performance $Q(t)$ from 0 to a given time T and the corresponding integral of a target system performance $\mathcal{T}Q(t)$ over the same time interval:

$$Res = E[Y], \tag{2}$$

where

$$Y = \frac{\int_0^T Q(t)dt}{\int_0^T \mathcal{T}Q(t)dt}. \tag{3}$$

Thereby, the system performance $Q(t)$ is a stochastic process. The target system performance $\mathcal{T}Q(t)$ can be generally considered as a stochastic process as well, however, for simplicity, $\mathcal{T}Q(t)$ may be assumed as a non-random and constant quantity $\mathcal{T}Q$. Assuming that the actual system performance does not exceed the target performance, the metric takes values between 0 and 1. For $Res = 1$, the system performance is equal to the target system performance, while $Res = 0$ indicates that the system is not functioning during the entire period under consideration.

2.2. Adapted Systemic Risk Measure

In [22], Feinstein et al. proposed a general approach to measuring systemic risk, e.g., pursued in finance [49]. In [20], this risk measure was adapted and extended for the application to engineering systems as summarized in this section. The adapted systemic risk measure comprises a descriptive input-output model and an acceptance criterion that represents normative resilience standards of a regulatory authority.

Let a system be given with m components $i \in \{1, \dots, m\}$ of type $k_i \in \{1, 2, \dots, K\} \subseteq \mathbb{N}$ with e properties that influence the system performance $Q(t)$. These properties, hereafter referred to as "endowment properties", affect system resilience and can be improved through capital allocations. Then, the component i is characterized by

$$\begin{aligned}(\boldsymbol{a}_i; k_i) = \\ (\eta_{i1}, \eta_{i2}, \dots, \eta_{ie}; k_i) \in \mathbb{R}^{(1\times e)} \times \mathbb{N},\end{aligned} \tag{4}$$

where $(\eta_{i1}, \eta_{i2}, \dots, \eta_{ie})$ are the numerical values of the e relevant endowment properties. Consequently, the entire system can be described by a tuple, consisting of the matrix $\boldsymbol{A} \in \mathbb{R}^{(m\times e)}$ and the column vector $\boldsymbol{z} \in \mathbb{N}^m$ that captures the component types:

$$(\boldsymbol{A}; \boldsymbol{z}) = \begin{pmatrix} \eta_{11} & \eta_{12} & \cdots & \eta_{1e}; & z_1 \\ \eta_{21} & \eta_{22} & \cdots & \eta_{2e}; & z_2 \\ \vdots & \vdots & & \vdots & \vdots \\ \eta_{m1} & \eta_{m2} & \cdots & \eta_{me}; & z_m \end{pmatrix}. \tag{5}$$

The system under consideration is defined via a descriptive, non-decreasing input-output model $Y = Y_{(\boldsymbol{A};\boldsymbol{z})}$ that is specified by this tuple and relates endowment properties to system performance. With respect to Eq. (2), the model output is specified as $Y = Y_{(\boldsymbol{A};\boldsymbol{z})}$ dependent on the current endowment allocation $(\boldsymbol{A}; \boldsymbol{z})$.

Further, consider the following specific acceptance set

$$\mathcal{A} = \{X \in \mathcal{X} \mid E[X] \geq \alpha\} \tag{6}$$

for a normalized model output X and its expected value $E[X]$ with $\alpha \in [0, 1]$. Correspondingly, the risk measure is defined as

$$R(Y) = \{\boldsymbol{A} \in \mathbb{R}^{m\times e} \mid Y_{(\boldsymbol{A};\boldsymbol{z})} \in \mathcal{A}\}, \tag{7}$$

that is the set of all endowment property allocations $\boldsymbol{A}$ such that the system reaches a resilience value greater or equal to α.

In practice, it might be necessary to impose structural restrictions on the matrix in Eq. (5). For example, consider the case that any component i of a specific type should be configured in the same way, i.e., the row vectors $\boldsymbol{a}_i$ are claimed to be equal. In [22], Feinstein et al. capture such constraints by monotonously increasing functions $g_z : \mathbb{R}^p \to \mathbb{R}^{(m\times e)}$, $a' \mapsto (A; z)$ with $z \in \mathbb{R}^m$ denoting the component types. Such a function maps a lower-dimensional set of parameters $a' \in \mathbb{R}^p$ to the system description given in Eq. (5).

2.3. Grid Search Algorithm and the Curse of Dimensionality

According to [22] and [20], the measure of systemic risk might be determined via a combination of a grid search algorithm and stochastic simulations. The grid search algorithm operates in the space of all possible endowments, while stochastic simulations are employed to evaluate system resilience for the endowment allocations according to the grid search algorithm. The probabilistic resilience metric (Eq. (2) and Eq. (3)) is estimated by means of Monte Carlo simulation. The grid search algorithm given in [22] consists of two phases and can be recapitulated as follows:

(I) Search along the main diagonal of the space of endowment properties until the first acceptable combination is found based on the adapted systemic risk measure.
(II) Identify the Pareto front between the set of acceptable endowments $R(Y)$ and its complement $R(Y)^c$ starting at the first accepted allocation.

The algorithm allows to compute the entirety of $R(Y)$ while significantly reducing the computational cost due to the assumed monotonicity property of the input-output model $Y_{(A;z)}$ given in Sec. 2.2. For a detailed description of a grid search algorithm for two dimensional problems, see [22], Ch. 4.

In [20] this algorithm was included in the resilience decision-making method and applied to case studies with two dimensional parameter spaces. In their work [22], Feinstein et al. point out that the grid search algorithm is applicable to higher dimensional problems "[...] *at the price of substantially larger computation times and required memory capacity.*". However, when analyzing real technical systems, it is often inevitable to consider a large number of influencing factors and thus a higher dimensionality of the parameter space. Therefore, in Sec. 5, an extension of the previously proposed resilience decision-making methodology to n-dimensional problems is applied to a four-dimensional functional model of an axial compressor and, in Sec. 7, as part of the novel methodology proposed in Sec. 4, it is applied to the *U-Bahn* and *S-Bahn* system of Berlin, addressing a five-dimensional problem.

3. Concept of Survival Signature

Introduced in [35], the concept of survival signature allows to compute the survival function of a system with multiple component types and attracted increasing attention for its advantageous features over the last decade. One of its merits is the high efficiency in repeated model evaluations due to the separation of the topological system reliability and the probability structure of system component failures. At the same time, the survival signature radically condenses information on topology. System components are of one type if their failure times are independent and identically distributed (*iid*) or exchangeable. This differentiation is important when it comes to modeling dependent component failure times [36]. A brief recap of the concept is provided in the following subsections. Detailed information about both the derivation of the concept and further applications can be found in [35, 36, 50].

3.1. Structure Function

Let a system be given consisting of m components of a single type. Further, let $\boldsymbol{x} = (x_1, x_2, \ldots, x_m) \in \{0, 1\}^m$ define the corresponding state vector of the m components, where $x_i = 1$ indicates a functioning state of the i-th component and $x_i = 0$ indicates a non-functioning state. Then, the structure function ϕ is a function of the state vector $\boldsymbol{x}$ defining the operating status of the considered system: $\phi = \phi(\boldsymbol{x}) : \{0, 1\}^m \to \{0, 1\}$. Accordingly, $\phi(\boldsymbol{x}) = 1$ denotes a functioning system and $\phi(\boldsymbol{x}) = 0$ specifies a non-functioning system.

Suppose that a system consists of components of more than one type, i.e., $K \geq 2$. Then, the quantity of system components is denoted by $m = \sum_{k=1}^{K} m_k$, where m_k is the number of components of type $k \in \{1, 2, \ldots, K\}$. Correspondingly, the state vector for each type is given by $\boldsymbol{x}^k = \left(x_1^k, x_2^k, \ldots, x_{m_k}^k\right)$.

3.2. Survival Signature

The survival signature summarizes the probability that a system is functioning as a function solely depending on the number of functioning components l_k per component type $k \in \{1, 2, \ldots, K\}$. Assuming the failure times within a component type to be *iid* or exchangeable, the survival signature is defined as:

$$\Phi(l_1, l_2, \ldots, l_K) = \left[\prod_{k=1}^{K} \binom{m_k}{l_k}^{-1}\right] \times \sum_{\boldsymbol{x}\in S_{l_1,l_2,\ldots,l_K}} \phi(\boldsymbol{x}), \qquad (8)$$

where $\binom{m_k}{l_k}$ corresponds to the total number of state vectors $\boldsymbol{x}^k$ of type k and $S_{l_1,l_2,\ldots,l_K}$ denotes the set of all state vectors of the entire system for which $l_k = \sum_{i=1}^{m_k} x_i^k$. Consequently, the survival signature depends only on the topological reliability of the system, independent of the time-dependent failure behavior of its components that is described in Sec. 3.3. For more information on claimed exchangeability in practice, see [36, 41].

3.3. Probability Structure

The probability structure of system components specifies the probability that a certain number of components of type k is functioning at time t. Accordingly, $C_k(t) \in \{0, 1, \ldots, m_k\}$ represents the number of components of type k in a functioning state at time t. Further, assume the probability distribution for

the failure times of type k to be known with $F_k(t)$, denoting the corresponding cumulative distribution function. Then,

$$P\left(\bigcap_{k=1}^{K}\{C_k(t)=l_k\}\right)=\prod_{k=1}^{K}P\left(C_k(t)=l_k\right)$$
$$=\prod_{k=1}^{K}\binom{m_k}{l_k}[F_k(t)]^{m_k-l_k}[1-F_k(t)]^{l_k} \tag{9}$$

describes the probability structure of the system, regardless of its topology.

3.4. Survival Function

The survival function describes the probability of a system being in a functioning state at time t and results from Sec. 3.2 and 3.3 as:

$$P\left(T_s>t\right)=\sum_{l_1=0}^{m_1}\dots\sum_{l_K=0}^{m_K}\Phi\left(l_1,l_2,\dots,l_K\right)$$
$$\times P\left(\bigcap_{k=1}^{K}\{C_k(t)=l_k\}\right), \tag{10}$$

where T_s denotes the random system failure time. Clearly, the concept of survival signature separates the time-independent topological reliability and the time-dependent probability structure. Thus, the survival signature, calculated once in a preprocessing step, can be reused for further evaluations of the survival function, which are necessary, for example, when analyzing a variety of different system configurations that affect the probability structure given a constant system topology. The survival signature can be stored in a matrix, thereby summarizing the topological reliability. The utilization of this matrix circumvents the repeated evaluation of the often computationally expensive structure function. Note that it is precisely these properties of the survival signature concept that provide an important advantage over conventional methods when system simulations need to be performed repeatedly [37]. In terms of computational demand, Monte Carlo simulation may be used to approximate the survival signature of large systems [40].

4. Proposed Methodology

In this section, the proposed methodology for computationally efficient resilience analysis in the context of complex substructured systems is illustrated. The approach integrates the concept of survival signature described in Sec. 3 into the resilience decision-making framework recapped in Sec. 2. First, the preparation of the complex system by means of a formalized substructuring approach is presented. Second, the novel methodology is proposed.

4.1. Definition of Substructured Systems

Assume a substructured system $\mathcal{S}$ that is composed of a set of subsystems and a set of components. The subsystems can again be comprised of further subsystems and components. This substructuring approach can be conducted for $L \geq 1$ levels of subsystems, where only components exist at level $L+1$. Components are directly associated with probability distributions describing their time-dependent probabilistic behavior. Note that the level 1 relates to the overall system level. Figure 3 illustrates the substructuring concept.

Let there be n^v subsystems $\mathcal{S}_1^v, \mathcal{S}_2^v, \dots, \mathcal{S}_{n^v}^v$ and m^v components $C_1^v, C_2^v, \dots, C_{m^v}^v$ at level $v = 1, 2, \dots, L$. During the analysis, the information on component behavior is propagated from level $L+1$ to level 1 before determining the state s^0 of the overall system $\mathcal{S}$ in dependence on various topological (sub)system structures. In the context of the resilience framework in Sec. 2, the state $s^0 \in S \subseteq \mathbb{R}^+$ with state space S of the overall system $\mathcal{S}$ corresponds to the system performance $Q(t)$ that is basis for the resilience measure Res, see Eq. (2). Note that multiple resilience analyses might be conducted for various $Q(t)$. The quantity s^0 indicates system functionality from an ordered perspective and depends on the functionality of its directly subordinate subsystems and components. Given level $v = 1, \dots, L$, the dependency of the (sub)system state s_j^v on the state vector $\boldsymbol{x}_j^v$ is modeled via the mapping $s_j^v = \phi_j^v(\boldsymbol{x}_j^v) \in \{0, 1\}$, where ϕ_j^v is a structure function, i.e., a topological rule for system functioning as presented in Sec. 3.1. The state vector is introduced as $\boldsymbol{x}_j^v = (s_1^w, s_2^w, \dots, s_{n_j^w}^w, c_1^w, c_2^w, \dots, c_{m_j^w}^w)$ for the j-th subsystem at level v with $j = 1, 2, \dots, n^v$ and $w = v + 1$. Thereby, $s_p^w, c_q^w \in \{0, 1\}$ denote the functionality of the p-th subsystem and q-th component, respectively. Further, n_j^w is the number of subsystems at level w contained in subsystem j at level v and $\sum_j^{n^v} n_j^w = n^w$. Analogously, m_j^w has the equivalent interpretation for components. At level $v = 1$, the notation reduces to $s^0 = \phi^0(\boldsymbol{x}^0)$. The state vectors at level L comprises only component states as $\boldsymbol{x}_j^L = (c_1^w, c_2^w, \dots, c_{m_j^w}^w)$ with $j = 1, 2, \dots, n^L$, $c_i^w \in \{0, 1\}$ and $w = L + 1$.

The probability distributions governing the component states c_i^v are assumed to be known as CDF $F_k(t)$ for given component type k according to Sec. 3.3. Note that different subsystems might rely on the same component types. The assumption $s_j^v, c_i^v \in \{0, 1\}$ is due to the fact that the concept of survival signature is based on a binary-state consideration. However, multiple researchers work on extensions of the concept to a discrete or continuous multi-state consideration, see e.g. [51, 52, 53, 54].

4.2. Extension of the Adapted Systemic Risk Measure

In the resilience analysis of complex, substructured systems, it may be important that endowments can be formally assigned not only to system components but to other system structures, such as subsystems. To enable the incorporation of such endowment assignments in the novel methodology, the adapted systemic risk measure, cf. Sec. 2.2, is extended as follows.

Let a system, in addition to its m components, be given with a total of n subsystems $j \in \{1, \dots, n\}$ of $b_j \in \{1, 2, \dots, B\} \subseteq \mathbb{N}$ types over all system levels L with d endowment properties that influence the system performance $Q(t)$. Then, the subsystem j is characterized by

$$(\mathcal{S}_j; b_j) = (\xi_{j1}, \xi_{j2}, \dots, \xi_{jd}; b_j) \in \mathbb{R}^{(1\times d)} \times \mathbb{N}, \tag{11}$$

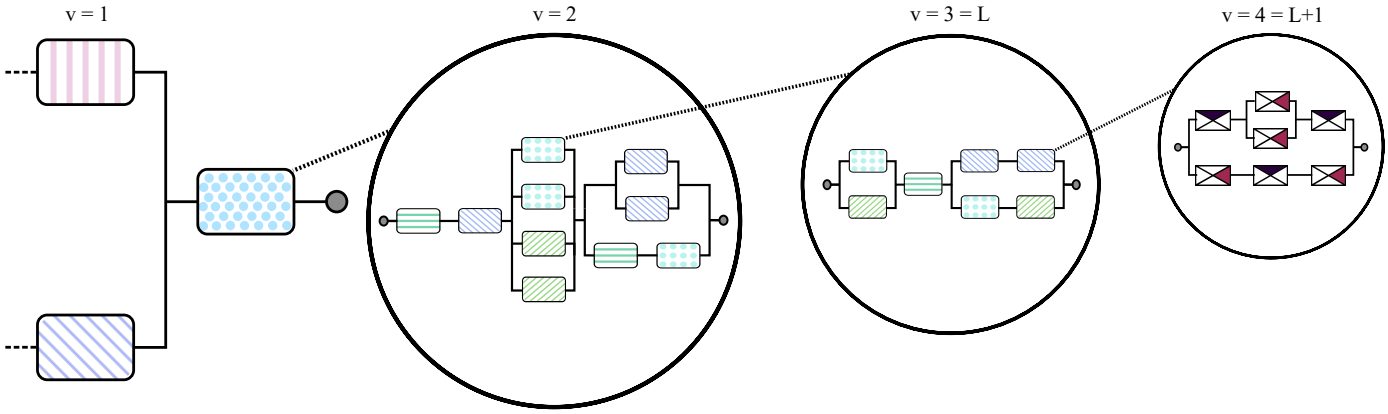

Figure 3: Illustration of the proposed substructuring concept.

where $(\xi_{j1}, \xi_{j2}, \ldots, \xi_{jd}; b_j)$ are the numerical values of the d relevant endowment properties. The entire system is then, in addition to the description by the tuple consisting of the matrix $\boldsymbol{A} \in \mathbb{R}^{(m \times e)}$ and the column vector $\boldsymbol{z} \in \mathbb{N}^m$, capturing the components, described by the tuple composed of the matrix $\boldsymbol{D} \in \mathbb{R}^{(n \times d)}$ and the column vector $\boldsymbol{h} \in \mathbb{N}^n$, capturing the subsystems:

$$(\boldsymbol{D}; \boldsymbol{h}) = \begin{pmatrix} \xi_{11} & \xi_{12} & \cdots & \xi_{1d}; & h_1 \\ \xi_{21} & \xi_{22} & \cdots & \xi_{2d}; & h_2 \\ \vdots & \vdots & & \vdots & \vdots \\ \xi_{n1} & \xi_{n2} & \cdots & \xi_{nd}; & h_n \end{pmatrix}. \tag{12}$$

The system under consideration is defined via the descriptive, non-decreasing input-output model $Y = Y_{(\boldsymbol{A};\boldsymbol{z}),(\boldsymbol{D};\boldsymbol{h})}$ that is specified by both tuples and relates endowment properties to system performance. Again, with respect to Eq. (2), the model output is specified as $Y = Y_{(\boldsymbol{A};\boldsymbol{z}),(\boldsymbol{D};\boldsymbol{h})}$ dependent on the current endowment allocation for components $(\boldsymbol{A}; \boldsymbol{z})$ and subsystems $(\boldsymbol{D}; \boldsymbol{h})$. Then, with the specific acceptance set $\mathcal{A}$ from Eq. 6, the extended adapted systemic risk measure is defined as

$$R(Y) = \left\{ \boldsymbol{A} \in \mathbb{R}^{m \times e}, \boldsymbol{D} \in \mathbb{R}^{(n \times d)} \mid Y_{(\boldsymbol{A};\boldsymbol{z}),(\boldsymbol{D};\boldsymbol{h})} \in \mathcal{A} \right\}, \tag{13}$$

that is the set of all endowment property allocations $\boldsymbol{A}$ and $\boldsymbol{D}$ such that the system reaches a resilience value greater or equal to α. Note that in this manner, equivalently, any performance-influencing endowments, of any system structures, or even endowments independent of system structures, can be incorporated into the resilience decision-making analysis.

4.3. Augmentation of the Resilience Analysis

The system resilience *Res* is governed by the reliability, robustness and recoverability of a system as illustrated in Fig. 1. The magnitude of these quantities is influenced by the endowment allocations that are captured in the tuples $(A; z)$ and $(D; h)$. The assigned resilience-enhancing endowment properties $(\eta_{i1}, \eta_{i2}, \ldots, \eta_{im})$ and $(\xi_{j1}, \xi_{j2}, \ldots, \xi_{jd})$ can either relate to a specific quantity or a subset of the three quantities and correspond to different implementations in the overall system performance model, i.e., input-output model $Y_{(A;z),(D;h)}$.

The reliability is typically the most computationally challenging quantity when evaluating system resilience *Res*. Thus, this part of the computation is augmented by the concept of survival signature with its advantageous separation and compact storage properties as well as the fundamental substructuring approach proposed in the previous Sec. 4.1 in order to enable efficient resilience analyses of large and highly complex systems.

In a pre-processing step, the survival signatures $\Phi_j^v(l_1, l_2, \ldots, l_K)$ of the $n = \sum_v^L n^v$ subsystems $\mathcal{S}_j^v$ are computed based on the corresponding structure functions ϕ_j^v as described in Sec. 3.2. Subsequently, the survival signatures are utilized to efficiently retrieve the topological subsystem reliability (online) for varying endowment configurations.

In order to identify the set of all acceptable endowments $R(Y)$, repeated evaluations of $Y_{(A;z),(D;h)}$ are required according to the grid search algorithm – various endowment allocations in the search space spanned over discretized numerical values of $A \in \mathbb{R}^{m \times e}$ with $m = \sum_v^{L+1} m^v$ and $D \in \mathbb{R}^{(n \times d)}$ with $n = \sum_v^{L+1} n^v$ need to be evaluated analogous to Sec. 2.3. In each evaluation N stochastic simulations of $Y_{(A;z),(D;h)}$ have to be performed to obtain $E[Y]$, see Eq. (2), and corresponding status assignments according to the acceptance set $\mathcal{A}$ in Eq. (6). Given the number of dimensions that need to be evaluated according to the grid search algorithm as M, the number of evaluations for $Q(t)$ is $M \cdot N \cdot u$ with u being the total number of time steps per simulation. Consequently, simulating system resilience is a complex, demanding and repeating challenge.

Computing the resilience directly relates to the computation of at least one structure function that can be any function that expresses the relation of interacting elements. The structure function can correspond to simple logical expressions, such as Reliability Block Diagrams (RBD) or fault trees, up to sophisticated simulation models, e.g., when assessing the network efficiency of a graph. In fact, such models often become extremely challenging in the context of real world systems. The evaluation of a global structure function including the entirety of all components at once might even be computationally unfeasible. In contrast, given a system in a substructered form $\mathcal{S}$ as proposed in Sec. 4.1, the computation of the system functional-

ity splits into the evaluation of multiple hierarchically ordered structure functions. Such a consideration enables a wider range of application in terms of system size and complexity, especially when the computational capacity is limited.

The computational efficiency is further enhanced by application of the survival signature. Given a system, substructered according to Sec. 4.1 with $L \geq 2$, the computation of subsystem reliabilities can be propagated from level L to level 1 by evaluating the survival functions of subsystems $\mathcal{S}_j^v$ based on the survival functions of $\mathcal{S}_p^w$ instead of computing $s_j^v = \phi_j^v(\boldsymbol{x}^v)$ for each level. Coolen et al. proposed a methodology to merge survival signatures of specifically arranged subsystems in the context of substructured systems [55]. However, note that this approach differs from the one developed in the current paper. The survival function $P(T_{s_j^v} > t)$ of the j-th subsystem at level v is then computed according to Eq. (10) w.r.t. the survival signature $\Phi_j^v(l_1, l_2, \ldots, l_K)$. At top-level 1, the failure rates of the subsystems $\mathcal{S}_j^1$ with $j = 1, 2, \ldots, n^1$, utilized to sample subsystem functionality, can then be obtained via the cumulative hazard function and its derivative:

$$\lambda^{s_j^1}(t) = -\frac{d \ln P(T_{s_j^1} > t)}{dt}. \tag{14}$$

This enables to sample the subsystem state s_j^1 for time step (t_h, t_{h+1}) online with significantly reduced computational effort when evaluating the system resilience Res. The computation of Res then only involves $n^1 + m^1$ instead of $\sum_v^{L+1} m^v$ elements. In addition, significantly increased computational efficiency is achieved due to the separation of system topology and probability structure, the latter determined by the current endowment allocation. While the component probability structure varies, the topological reliability, independent of the endowment allocation, is captured in the survival signature in a compact manner and can be retrieved repeatedly with close to no costs. Note that subsystems of the same type share the same survival signature. This can be exploited for increased efficiency as well. In fact, the computational advantage of the proposed approach scales with size and complexity of the considered system $\mathcal{S}$. The developed and employed algorithm is outlined in Alg. 4.3 for illustrative purposes.

In order to prove efficiency and general applicability, the novel approach is applied to an arbitrary complex system in Sec. 6 and to the *U-Bahn* and *S-Bahn* system of Berlin in Sec. 7.

Algorithm 4.3.

Step A Computation of the survival signatures for all subsystem $\mathcal{S}_j^v$ with $v = 1, 2, \ldots, L$ and $j = 1, 2, \ldots, n^v$.

Step B Identification of the Pareto front by executing the grid search algorithm; each endowment allocation is evaluated by performing the following steps:

Step B1. Generation of the failure rate matrix with dimensions $n^1 \times T$ based on Eq. (14) for each subsystem and each timestep t_h with $h = 1, 2, \ldots, u$ and generation of the failure rate matrix with dimensions $m^1 \times T$ for each component and each timestep; if $L \geq 2$, the failure rate matrix for $v = 1$ for each subsystem is generated recursively from bottom to top by computing the survival functions.

Step B2. Perform N samples with time $t_h = 0$:

a) Evaluate the system performance $Q(t_h)$.

b) Sample possible failures of subsystems $\mathcal{S}_j^1$ for $j = 1, 2, \ldots, n^1$ and components C_i^1 for $i = 1, 2, \ldots, m^1$ based on the failure rate matrices computed in Step B1.

c) Check if any failed subsystem/component has recovered; if a subsystem/component recovers, set the time counter of its specific failure rate to 0.

d) Set $t_h = t_{h+1} = t_h + \Delta t$ and repeat Steps a) – d) until $t_h = T$, i.e., the maximum time is reached.

Step B3. Obtain Res for the current endowment configuration via Eq. (2) and Eq. (3) over all time steps u and all samples N.

The complete algorithm has been implemented in the Julia package *ResilienceDecisionMaking.jl* and made publicly available on Github [56].

5. Multistage High-Speed Axial Compressor

Axial compressors are complex, multi-component key elements of gas turbines. Therefore, it is critical in both design and maintenance to consider as many factors affecting system performance as possible to efficiently maximize compressor resilience. To address this challenge, the decision-making analysis proposed in [20] regarding system resilience is extended in order to deal with components, respectively factors, of different types.

5.1. Model

In [57], the authors present a functional model of a four-stage high-speed axial compressor from the Institute of Turbomachinery and Fluid Dynamics at Leibniz Universität Hannover, Germany, depicting its functionality as well as reliability characteristics. For detailed information about this particular axial compressor see [58, 59, 60].

The model captures the dependence of the overall performance of the compressor, i.e., the total-to-total pressure ratio and the total-to-total isentropic efficiency, on the surface roughness of the individual blades. These are arranged in rotor and stator rows. The model is based on the results of a sensitivity analysis of an aerodynamic model of the compressor and the so-called Relative Important Indices, cf. [50]. A network representation of the functional model is shown in Fig. 4. Each component represents either a stator (S1 - S4) or rotor (R1 - R4) row.

The rows are classified into $K = 4$ component types $k_i \in \{1, 2, 3, 4\}\ \forall i \in \{1, \ldots, 8\}$. This classification, as well as the arrangement of the components, is based on the resulting effect of their blade roughness on the two performance parameters of the compressor. More precisely, an interruption between start and end implies that a roughness-induced performance

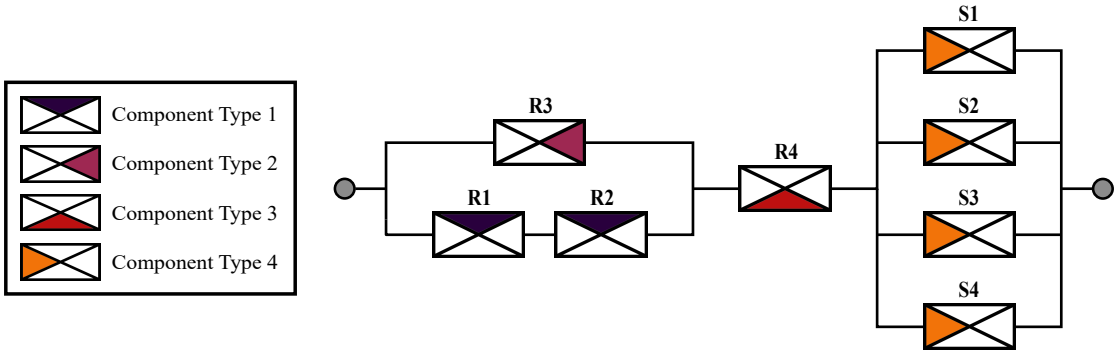

Figure 4: Functional model of the multistage high-speed axial compressor.

variation of at least 25% is exceeded, corresponding to a non-functional compressor. This defines the system performance $Q(t)$ of the functional model for subsequent application of the resilience decision-making method. The system performance is determined at each time point t_h and is 1 if there is a path from start to end and 0 if this connection is interrupted. More detailed information about the functional model and its derivation can be obtained from [57].

For the resilience analysis, it is assumed that each row, i.e., each component of the functional model, is characterized by two endowment properties, a roughness resistance *re* and a recovery improvement *rec*, such that a component is fully described by $(a_i; k_i) = (re_i, rec_i; k_i)$. In this context, the roughness resistance can be interpreted as a qualitative coating that counteracts the roughening of the blade surfaces. Both the roughness resistance re_i and the recovery improvement rec_i of each row i are assumed to be functions of the component type k_i, i.e., $re_i = re_{i'}$, $rec_i = rec_{i'}$ if $k_i = k_{i'}$.

Each component of the functional model can fail randomly after system performance is calculated at time t_h. A failed component is considered as no longer being part of the model and does not contribute to the overall system performance at time t_{h+1} and at all subsequent times until it is completely recovered. The failure probability of a component i in the time interval (t_h, t_{h+1}) is assumed to be constant in time, cf. [57], and is specified by

$$P\{(a_i; k_i) \text{ fails during } (t_h, t_{h+1})\} = \Delta t \cdot \lambda_i \tag{15}$$

with

$$\lambda_i = 0.8 - 0.03 \cdot re_i, \tag{16}$$

where λ_i is the time-independent failure rate. Increasing the roughness resistance of a blade row reduces the degradation of the surface and consequently the corresponding failure rate λ_i.

When a component i fails, its functionality is assumed to be immediately and completely recovered after a certain number of time steps, according to

$$r = r_{max} - rec_i \quad \text{with} \quad rec_i < r_{max} \tag{17}$$

where r_{max} is an upper bound on the number of time steps for recovery and rec_i is the recovery improvement that reduces the recovery duration. Note, that this recovery model corresponds to a one-step recovery profile and various alternative characteristic profiles of recovery are possible as well, cf., [16] and [4].

5.2. Costs of Endowment Properties

Optimal endowment properties are related to the quality of the components, and an increase in their production quality is associated with increasing costs. This should be taken into account in resilience decision-making. As discussed in [61], increasing the reliability of components in complex networks can be associated with an exponential increase in cost.

Increasing the endowment property of roughness resistance reduces the failure rate of blades in a row and thus improves reliability, see Eq. (15) and Eq. (16). Thus, its total cost is assumed to be

$$cost^{re} = \sum_{i=1}^{8} price^{re}_{(re_i;k_i)} \cdot 1.2^{(re_i - 1)}, \tag{18}$$

where re_i is the roughness resistance value of component i, k_i its type and $price^{re}_{(re_i;k_i)}$ an arbitrary common basic price. Accordingly an exponential relationship is assumed for the cost associated with recovery improvement:

$$cost^{rec} = \sum_{i=1}^{8} price^{rec}_{(rec;k_i)} \cdot 1.2^{(rec_i - 1)}. \tag{19}$$

The total cost $cost_{(A;z)}$ of an endowment is the sum of these costs:

$$cost_{(A;z)} = cost^{re} + cost^{rec}. \tag{20}$$

5.3. Scenario

In order to apply the decision-making method for resilience-enhancing endowments to the multistage high-speed axial compressor, the model parameter values and simulation parameter values shown in Tab. 1 are considered.

In a first step, the set of all acceptable endowments corresponding to a resilience value of at least $Res = 0.85$ over the considered time period is determined. Since any axial compressor blade improvement involves costs, the second step is to identify the most cost-efficient acceptable endowment, denoted as $\hat{A}$. The recovery improvement *rec* is assumed to be fixed for all components, regardless of the type, $rec_i = 11\ \forall i \in \{1, \ldots, m\}$ and the roughness resistance *re* is examined over $re_i \in \{1, \ldots, 20\}\ \forall i \in \{1, \ldots, m\}$. The roughness resistance values may be interpreted in ascending order as increasing quality levels of coatings.

Parameter	Scenario
Acceptance threshold α	0.85
Number of time steps u	200
Length of a time step Δt	0.05
Maximum time T	10
Base failure rate λ	0.8
Roughness resistance re	$re_i \in \{1, \dots, 20\}$
Roughness resistance price:	
$price^{re}_{(re_i;k_i)}$	800€ $\forall k_i \in \{1, 2, 3\}$
	500€ $\forall k_i = 4$
Maximum recovery time r_{max}	21
Recovery improvement rec	11
Recovery improvement price:	
$price^{rec}_{(rec;k_i)}$	600€
Sample size N	500

Table 1: Parameter values for the resilience decision-making method for the functional model of the multistage high-speed axial compressor.

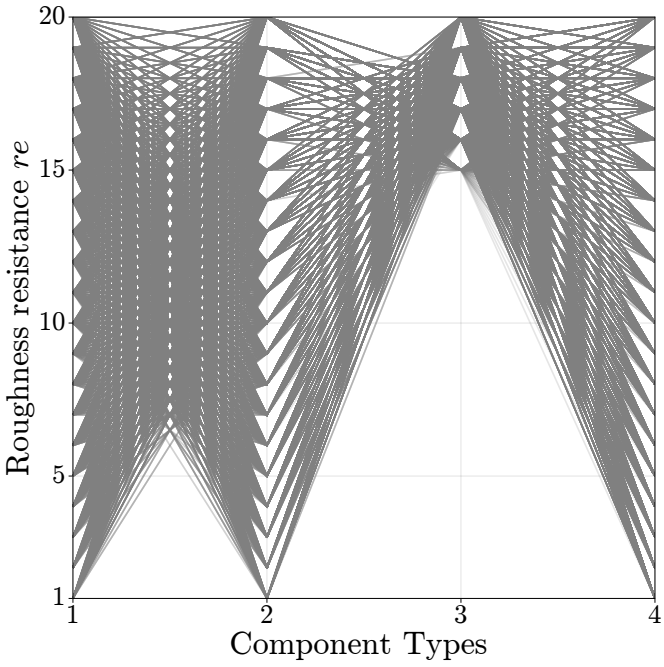

Figure 5: Numerical results of the 4D grid search algorithm for the functional model of the axial compressor with explored roughness resistance values.

Figure 5 illustrates the results of the grid search algorithm. It shows the roughness resistance combinations contained in $R(Y)$, i.e., all combinations that lead to a satisfying system resilience of at least $Res = 0.85$. It can be clearly seen that the roughness resistance of the blades of the fourth stage (component type 3) has the greatest influence on the system resilience. Combinations with coating qualities of $re_i \leq 15$ at the fourth stage are generally not sufficient to achieve an acceptable level of resilience, regardless of the endowment property values of the other component types. In addition, the roughness resistance of the four stators (component type 4) has the least influence on system resilience of all types. Here, a minimum coating quality of $re_i = 1$ as endowment is in various combinations already sufficient to achieve acceptable resilience values. The same applies to the rotors of component type 1 and type 2. However, the components of the other types require significantly higher coating qualities compared to the stators in order to compensate for the small roughness resistance values in these both types.

The design, maintenance and optimization of complex systems, such as an axial compressor, are invariably subject to monetary limitations. It is crucial for decision-making to be able to take these financial constraints into account. Therefore, Fig. 6 shows only those roughness resistance combinations included in $R(Y)$ that result in an acceptable system resilience of at least $Res = 0.85$ and are less expensive than a predefined cost limit for the total roughness resistance, that is arbitrarily assumed to be $cost^{re} = 40\,000$€ in this case study.

The results reveal that only configurations with low coating qualities for stators (component type 4) are below the cost limit. On the one hand, this is due to their aforementioned low influence on system resilience, and on the other hand to the high cost of the quality levels for the stators. Although the base price of 500€ is rather low, it is significantly higher in terms of cost for the entire component type than for the other types due to the higher total number of components of this type. In addition, only configurations that provide the highest quality levels of $re_i \geq 18$ for the type 3 rotor are acceptable and below the price limit. The roughness resistance of this rotor has such a large impact on system resilience that at lower quality levels, compensation by higher quality levels of the remaining stages would exceed the given budget. Although the roughness resistance of the rotor of component type 2 has a lower influence on the system resilience than that of component type 3, minimal quality levels of the coating can not be compensated by high qualities of the other components. Therefore, at least $re_i = 5$ for $k_i = 2$ is required to fulfill the acceptance criterion.

The grid search algorithm is able to reduce the numerical effort for the calculation of $R(Y)$ by about 98%. As a result, only 2% of the potential combinations of roughness resistance values need to be evaluated.

Taking into account the base prices in Tab. 1, the most cost-efficient endowment is characterized by roughness resistances of $re_i = 7$ for $k_i = 1$, $re_i = 13$ for $k_i = 2$, $re_i = 19$ for $k_i = 3$ and $re_i = 1$ for $k_i = 4$ for the respective components. In Fig. 6 the corresponding configuration is highlighted in blue. The final cost results from Eq. (20) as $cost_{(\hat{A};z)} = cost^{re} + cost^{rec} = 35\,209$€ + 29 720€ = 64 929€.

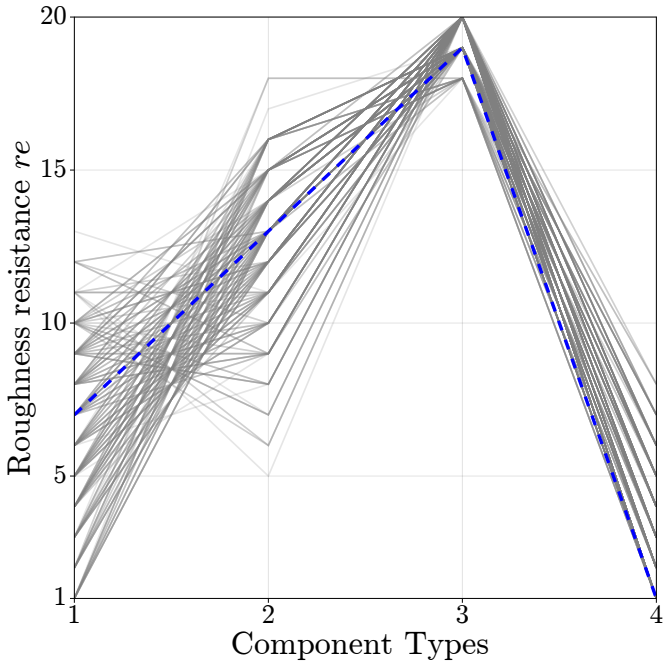

Figure 6: Numerical results of the 4D grid search algorithm for the functional model of the axial compressor with explored roughness resistance values and a cost threshold for roughness resistance of 40 000€.

6. Complex System

In [37] and [41] the authors apply their introduced simulation approaches for reliability analysis on an arbitrary complex system. In order to demonstrate the wide applicability and efficiency of the proposed methodology developed in this paper, this complex system is considered, adapted by means of substructuring, and an efficient resilience decision-making analysis is conducted.

6.1. Model

The arbitrary complex system consists of $n = 14$ subsystems, each assigned to one of $B = 6$ subsystem types. Figure 7 illustrates the complex system and the assignment of subsystems to their types. A connection between start node and target node indicates a functioning state and an interruption of this connection indicates a non-functioning state of the overall system. This defines the system performance $Q(t)$ of the functional model for subsequent application of the resilience decision-making method. The system performance is determined at each time point t_h and is 1 if there is a path from start to end and 0 if this connection is interrupted. Note that the complex system is thus formally an RBD. For illustration and simplicity, it is assumed that there is only one level of subsystems, i.e., $l = L = 1$, and thus $\boldsymbol{x}^s = (s_1, s_2, \ldots, s_{14})$, $\mathcal{S}_j^1 = \mathcal{S}_j$, and $\lambda^{s_j^1}(t) = \lambda^{s_j}(t)$. Figure 8 illustrates the structure of the six subsystem types. These are formally RBDs as well. It is assumed that each subsystem of the same type is represented by the same RBD. A subsystem $\mathcal{S}_j$ is considered to be functional if a connection exists from start to end and non-functional if this connection is interrupted, i.e., $s_j \in \{0, 1\}\ \forall j \in \{1, \ldots, 14\}$. Depending on the type, the subsystems consist of seven to ten components. Thus, the overall system is composed of $m = 106$ individual components.

The components are classified into $K = 2$ types $k_i \in \{1, 2\}$ $\forall i \in \{1, \ldots, 106\}$, i.e., 50 components of type 1 and 56 components of type 2. For the resilience analysis, each component of the model, is assumed to be characterized by an endowment property, that is the reliability improvement *rel*, such that a component is fully described by $(a_i; k_i) = (rel_i; k_i)$. Note that the reliability improvement rel_i of each component i is assumed to be function of the component type k_i, i.e., $rel_i = rel_{i'}$ if $k_i = k_{i'}$. Further, each component type, and thus each component, is characterized by a specific time-dependent failure behavior. In practice, the underlying distribution functions, describing this behavior, need to be derived from existing operational data. However, the consideration of real data is often highly challenging due to the inherent uncertainty caused by, e.g., lack of data, measurement inaccuracies, subjective expert knowledge, small sample sizes, etc. New developments in the context of the survival signature as introduced, e.g., in [41], allow for the efficient consideration and propagation of uncertainties through the entire model. They will be incorporated into the proposed methodology towards an imprecise resilience approach in future work of the authors. However, for the purpose of proof of concept and applicability, exponential distributions are considered for both component types in this case study as

$$F_i(t; \lambda_i(rel_i)) = 1 - e^{-\lambda_i(rel_i)t} \text{ for } t \geq 0, \tag{21}$$

with

$$\lambda_i(rel_i) = \lambda_{i,\max} - \Delta\lambda_i \cdot rel_i, \tag{22}$$

being the failure rate of component i of type k depending on the corresponding reliability improvement rel_i. $\lambda_{i,\max}$ is the maximum failure rate and $\Delta\lambda_i$ denotes the failure rate reduction per reliability improvement rel_i that is assumed to be constant for each component type, leading to equidistant failure rate variations.

The simulation can be summarized as follows: after the system performance has been computed at time t_h, each subsystem $\mathcal{S}_j$ of the complex system can fail at random based on the extracted and time-dependent failure rate $\lambda^{s_j}(t_h)$ from corresponding survival function, cf. Eq. (14). A failed subsystem is treated as no longer present in the model and does not contribute to the overall system performance $Q(t)$ at time t_{h+1} and all subsequent time points until it is fully recovered. The failure probability of a subsystem $\mathcal{S}_j$ in the time interval (t_h, t_{h+1}) is

$$P\left\{\mathcal{S}_j \text{ fails during } (t_h, t_{h+1})\right\} = \Delta t \cdot \lambda^{s_j}(t_h). \tag{23}$$

If a subsystem $\mathcal{S}_j$ failed, its functionality is assumed to be immediately and fully recovered after r time steps, again corresponding to a one-step recovery profile. It is assumed that a repaired subsystem and thus all components of the subsystem are in as-new original condition after repair. Note that this is an assumption for the sake of demonstration, and in reality deviating states might be obtained after repair, possibly depending on further endowment properties that affect the duration and quality

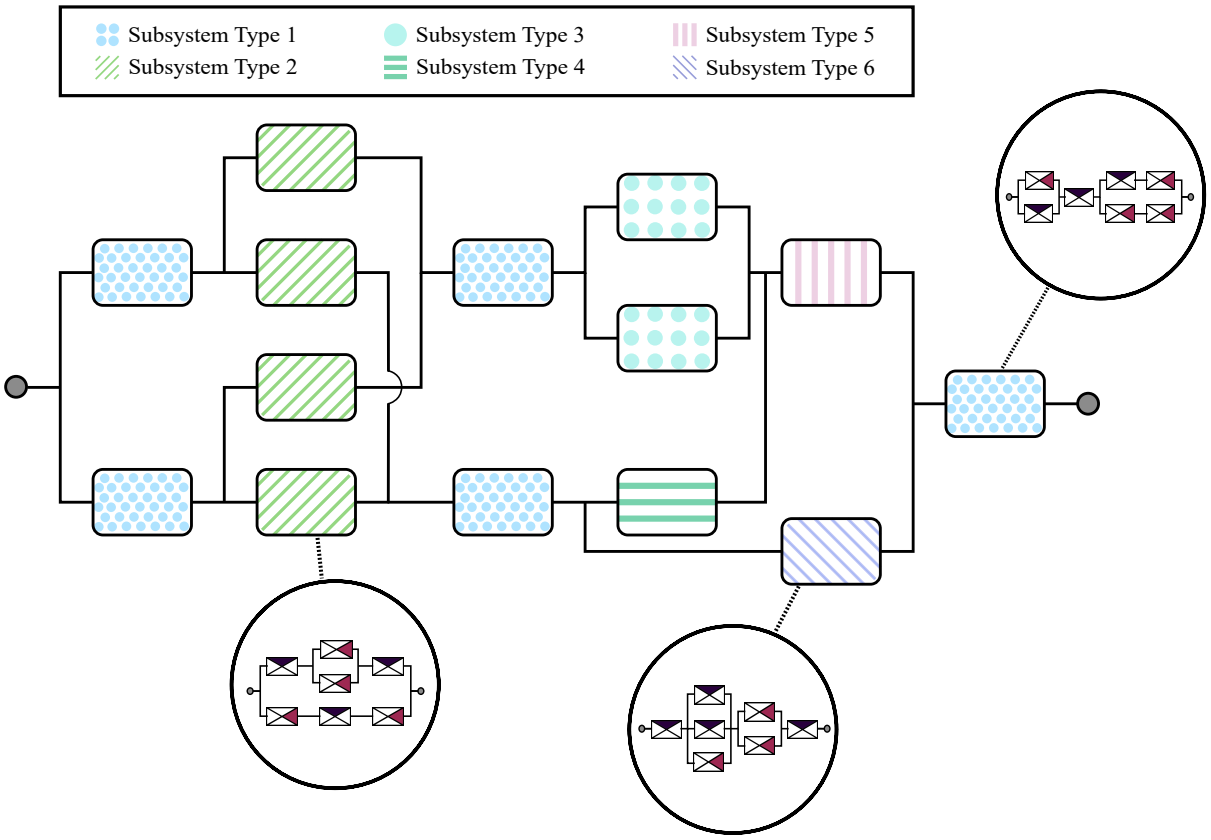

Figure 7: Representation of the arbitrary complex system with 14 components, adapted from [37].

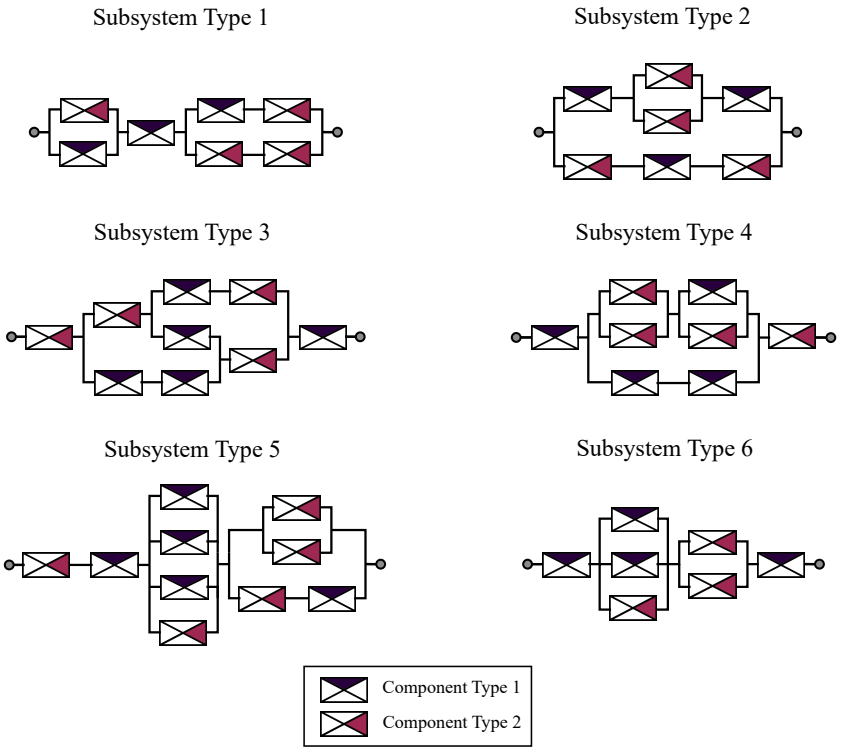

Figure 8: Representation of the $B = 6$ subsystem types of the complex system.

of recovery. After recovery, the survival function of a subsystem is time-zeroed, such that the resulting failure rate per simulation step $\lambda^{s_j}(t_h)$ evolves over time equivalent to that of a subsystem in new condition.

6.2. Costs of Endowment Properties

The improvement of endowment properties is inevitably associated with costs. Increasing the endowment property "reliability improvement" reduces the failure rate of components and consequently of corresponding subsystems. Again, an exponential relationship between costs and improvements is assumed. Then the total costs can be defined as

$$cost_{(A;z)} = cost^{rel} = \sum_{i=1}^{106} price^{rel}_{(rel_i;k_i)} \cdot 1.2^{(rel_i-1)}, \qquad (24)$$

where $(rel_i; k_i)$ is the reliability improvement value of component i, k_i its type and $price^{rel}_{(rel_i;k_i)}$ is an arbitrary common basic price.

6.3. Scenario

The considered model parameters and simulation parameters values for the application of the resilience decision-making method for complex and substructured systems to the arbitrary complex system illustrated in Fig. 7, are shown in Tab. 2. The recovery is assumed to be fixed with $r = 20$ time steps for all subsystems, regardless of the type. The reliability improvement rel_i is explored over $rel_i \in \{1, \dots, 10\}\ \forall i \in \{1, \dots, m\}$.

In a pre-processing step, the survival signatures of all 14 subsystems are determined. As an example, Tab. 3 depicts the survival signature values of subsystem type 5 of the complex system. For clarity, only the non-trivial survival signature values are shown, i.e., all values that are neither zero or one. Then the analysis starts as follows: In a first step, the set of all acceptable endowment configurations $R(Y)$, corresponding to a resilience value of at least $Res = 0.9$ over the considered time period, is determined according to Algorithm 4.3. Since any improvement of the system components is associated with costs, the second step is to identify the most cost-efficient acceptable endowment $\hat{A}$.

Figure 9 illustrates the results of the grid search algorithm. It shows the reliability improvement combinations contained in $R(Y)$, i.e. all combinations that lead to a satisfying system resilience. It can be seen, that the reliability improvement of components of type 1 is more important, i.e., has a higher impact on the overall system resilience than the reliability improvement of components of type 2. For maximum reliability improvement values for type 1, i.e., $rel_i = 10$ for $k_i = 1$, even low reliability improvement values for type 2, i.e., $rel_i = 2$ for $k_i = 2$, are sufficient in order to fulfill the acceptance criterion and reach system resilience values of at least $Res = 0.90$. On the other hand, with maximum reliability improvement for components of type 2, i.e., $rel_i = 10$ for $k_i = 2$, a moderate reliability improvement for type 1 of at least $rel_i = 4$ for $k_i = 1$ is required to meet the acceptance criterion.

These results are plausible, since a detailed examination of the subsystem types and their topology, cf. Fig. 8, reveals that components of type 1 hold a total of six so-called bottleneck

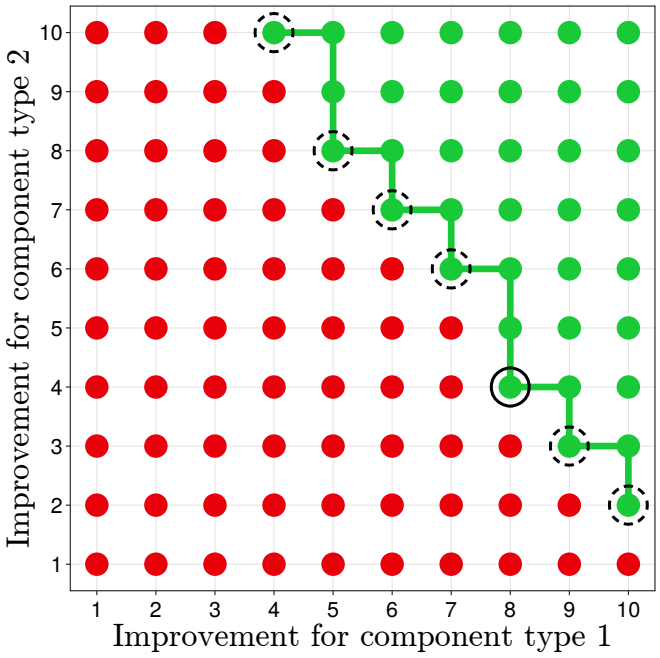

Figure 9: Numerical results of the 2D grid search algorithm for the complex system with explored reliability improvement values.

positions within the subsystems, i.e., positions where the failure of a single component interrupts the functioning of the entire subsystem, while components of type 2 occupy only three of these positions. This results in a higher influence of component type 1 on the functionality of the subsystems and thus ultimately in a higher influence on overall system resilience. Accordingly, the quality of reliability improvement of component type 1 is more relevant than that of component type 2. Looking at the probabilistic structure of the components, it is noticeable that the failure rate reduction for components of type 2 is greater than for components of type 1, i.e., the increase in reliability improvement for type 2 probabilistically generates a higher surplus value compared to improvements of type 1. However, this obviously cannot balance the influence gradient between both types and thus underlines the critical topological importance of type 1 components.

The design, maintenance and optimization of complex systems is typically restricted by economic limitations. It is crucial for decision-making to be able to take these monetary constraints into account. Assuming the arbitrary base prices in Tab. 2, the most cost-effective acceptable endowment $\hat{A}$ is specified by a reliability improvement configuration of $rel_i = 8$ for $k_i = 1$ and $rel_i = 4$ for $k_i = 2$ for the respective components. In Fig. 9, the corresponding configuration is highlighted. Note that due to the monotonicity of the input-output model and the monotonically increasing endowment costs, the most cost-efficient endowment can only be located on the dominant vertices of the Pareto front. Therefore, only these configurations need to be examined in terms of cost. The final cost results from Eq. (24) as $cost_{(\hat{A};z)} = 372\,695$€.

Due to the utilization of the grid search algorithm, the numer-

Table 2: Parameter values for the resilience decision-making method on the arbitrary complex system.

Parameter	Scenario
Acceptance threshold α	0.90
Number of time steps u	200
Length of time step Δt	0.05
Maximum time T	10
Maximum failure rate $\lambda_{i,\max}$	$\lambda_{i,\max} = 0.15$ for $k_i = 1$ $\lambda_{i,\max} = 0.20$ for $k_i = 2$
Failure rate reduction $\Delta\lambda_i$	$\Delta\lambda_i = 0.014$ for $k_i = 1$ $\Delta\lambda_i = 0.019$ for $k_i = 2$
Reliability improvement rel_i	$rel_i \in \{1, \ldots, 10\}$ for $k_i \in \{1, 2\}$
Reliability improvement price $price^{rel}_{(rel_i;k_i)}$	$price^{rel}_{(rel_i;1)} = 1\,000$€ $price^{rel}_{(rel_i;2)} = 2\,000$€
Recovery time steps r	20
Sample size N	500

Table 3: Non-trivial survival signature values of subsystems with $b_j = 5$ of the complex system, shown in Fig. 7 and Fig. 8.

l_1	l_2	$\Phi(l_1, l_2)$
2	4	1/25
3	3	3/50
2	5	3/25
4	3	3/20
3	4	9/50
2	6	1/5
5	3	11/50
6	3	3/10
3	5	3/10
4	4	33/100
3	6	2/5
5	4	23/50
4	5	12/25
6	4	3/5
4	6	3/5
5	5	16/25
6	5	4/5
5	6	4/5

ical effort required to compute $R(Y)$ is reduced. Only 23% of all possible configurations of reliability improvement values need to be evaluated. This reduction effect scales with the size and dimensionality of the endowment search space. By means of the novel resilience decision-making method, the considered complex system could be reduced from its entirety of 106 individual components to 14 components on the top-level with respect to the resilience analysis and the associated identification of all acceptable endowment configurations, which drastically reduces the computational effort. Nevertheless, all 106 components and their influence were considered by incorporating and propagating the subsystems' survival functions. Again, this effect scales with increasing complexity and size of the investigated systems.

7. *U-Bahn* and *S-Bahn* System of Berlin

About two thirds of the total of 1.5 billion passengers per year are transported by Berlin's subway U-Bahn and suburban trains S-Bahn [62, 63], making these two transport services the most used means of public transport in Berlin and thus of utmost importance for the German capital. Key infrastructures that are of such significant social and economic relevance to modern societies obviously and inevitably need to be as resilient as humanly possible. The applicability of the methodology developed in this work to large complex systems is demonstrated on a comprehensive model of the Berlin U-Bahn and S-Bahn system. The objective is to identify suitable resilience-enhancing properties for all stations in the system, taking into account monetary constraints. This allows the characterization of acceptable endowments for the system in terms of reliability, robustness, and recoverability. This approach can be applied not only to any phase during the life cycle of existing systems, but also to systems in the design phase, in order to optimize their resilience.

7.1. Model

Berlin's U-Bahn and S-Bahn systems are highly interconnected systems that are linked by numerous stations. According to [64], they may therefore be considered as a unified system,

hereafter referred to as "metro system". In [20] the authors apply their introduced approach for resilience decision-making to a model of the Berlin metro system. In order to demonstrate the wide applicability and efficiency of the proposed methodology developed in this work, this model is considered, extended and adapted by means of substructuring, and an efficient and multi-dimensional resilience decision-making analysis is conducted.

In [65], Zhang et al. proposed how mapping of metro networks into topological graphs can be conducted. Based on this, the Berlin metro system consists of 306 nodes for 306 metro stations and 350 edges for 350 connections between these stations. For simplicity, parallel connections are mapped to single edges in the model, and are assumed to be undirected. These assumptions reduce the complexity of the metro system. Figure 10 illustrates the graph representation.

The functionality of systems depends on the functionality of its components. However, the functionality of these components often depends again on the functionality of a variety of subcomponents, etc. A major challenge in modeling is therefore determining an appropriate level of detail.

The resilience decision-making methodology proposed in this paper allows for the incorporation of such subsystem structures by live propagation of corresponding reliability characteristics up to the top-level. Therefore, for the resilience analysis of the metro system, each metro station is modeled as a subsystem with own functionality and performance function. Again, for illustrative purposes and sake of convenience, assume that there is only one level of subsystems, i.e., $l = L = 1$, and thus $\boldsymbol{x}^s = (s_1, s_2, \ldots, s_{306})$, $\mathcal{S}_j^1 = \mathcal{S}_j$ and $\lambda^{s_j^1}(t) = \lambda^{s_j}(t)$ with $n = 306$ subsystems respectively metro stations.

In terms of reliability modeling, subcomponents could correspond to structural elements, such as stairs, columns, ceilings, station rails as well as electric facilities, such as railway power supply, elevators, escalators, ventilation plants, information systems and illuminations. These subcomponents can be subdivided in terms of their functionality and relevance to the metro station, such as in rail operations related components and user accessibility related components. For illustrative purpose, the analysis is restricted to reliability modeling of metro stations. Therefore, functional models are defined for the metro station subsystems that are, as in the previous case study, formally RBDs. Again, a subsystem $\mathcal{S}_j$ is considered to be functional if a connection from start to end exists and non-functional if this connection is interrupted, i.e., $s_j \in \{0, 1\}\ \forall j \in \{1, \ldots, 306\}$. Figure 10 illustrates three of these subsystems for three different metro stations as an example. The metro stations are classified into $B = 6$ types, depending on the number of their connections to direct neighbors, i.e., stations with only one connection form subsystem type 1, stations with two direct neighbors form subsystem type 2, etc. For the analysis, each subsystem is assumed to be characterized by an endowment property, that is the recovery improvement *rec*, such that a metro station j with type b_j is described by $(\mathcal{S}_j; b_j) = (rec_j; b_j)$. Note, that the recovery improvement rec_j of each metro station is assumed to be a function of the station type b_j, i.e., $rec_j = rec_{j'}$ if $b_j = b_{j'}$. For simplicity, it is assumed that each metro station of a type is represented by the same RBD. Figure 11 displays the structure of all six subsystem types and Fig. 12 tabulates the number of individual metro stations per type.

Depending on the type and thus with increasing complexity related to the number of direct neighbors, also known as node degree, the subsystems consist of four up to twenty-one components. Taking into account the information from Fig. 12, the overall system therefore consists of a total of $m = 2776$ considered individual components.

The components are classified into $K = 4$ types $k_i \in \{1, 2, 3, 4\}\ \forall i \in \{1, \ldots, 2776\}$. For the analysis, each component is assumed to be characterized by an endowment property, that is the reliability improvement *rel*, such that a component is fully described by $(a_i; k_i) = (rel_i; k_i)$. Note, that the reliability improvement rel_i of each component is assumed to be a function of the component type k_i, i.e., $rel_i = rel_{i'}$ if $k_i = k_{i'}$. Further, each component is characterized by a specific time-dependent failure behavior. For the purpose of proof of concept and applicability, for component type 1 and 3, i.e., $k_i = 1$ and $k_i = 3$, exponential distributions are considered according to Eq. (21) and Eq. (22). For component type 2 and 4, i.e., $k_i = 2$ and $k_i = 4$, two parametric gamma distributions are considered. The cumulative distribution function of the gamma distribution can be derived based on its probability density function that is given in terms of the rate parameter $\lambda_i(rel_i)$ depending on the current reliability endowment value rel_i of component i of type k_i as

$$f(t; \alpha_i, \lambda_i(rel_i)) = \frac{t^{\alpha_i - 1} e^{-\lambda_i(rel_i)t} \lambda_i(rel_i)^{\alpha_i}}{\Gamma(\alpha_i)}, \tag{25}$$

for $t, \alpha_i, \lambda_i(rel_i) > 0$, where α_i is the shape parameter, $\lambda_i(rel_i)$ is the rate parameter, and $\Gamma(\alpha_i)$ is the well-known Gamma function. Consequently, the cumulative distribution function can be obtained by integration and with respect to the current endowment of component i it can be formulated as

$$F(t; \alpha_i, \lambda_i(rel_i)) = \int_0^t f(u; \alpha_i, \lambda_i(rel_i))du. \tag{26}$$

$\lambda_i(rel_i)$ is again a function of the component specific reliability improvement and given by Eq. (22).

In order to perform a resilience analysis, the definition of an appropriate system performance measure for the metro system is imperative. As in [65] and [20], in this case study, the so-called network efficiency E_f is adopted as the relevant performance measure, i.e., $Q(t) = E_f(t)$. Zhang et al. justified in [65] their choice by stating that connectivity between individual metro stations is an essential criterion for evaluating metro operations. As described by Latora and Marchiori in [66], network efficiency is a quantitative indicator of network connectivity and is defined as:

$$E_f = \frac{1}{n(n-1)} \sum_{u \neq v} \frac{1}{d_{uv}} \tag{27}$$

with n the number of subsystems, i.e., metro stations in the network and d_{uv} the path length between metro station u and metro station v, i.e., the shortest distance between these stations. A comprehensive overview of algorithms to efficiently determining

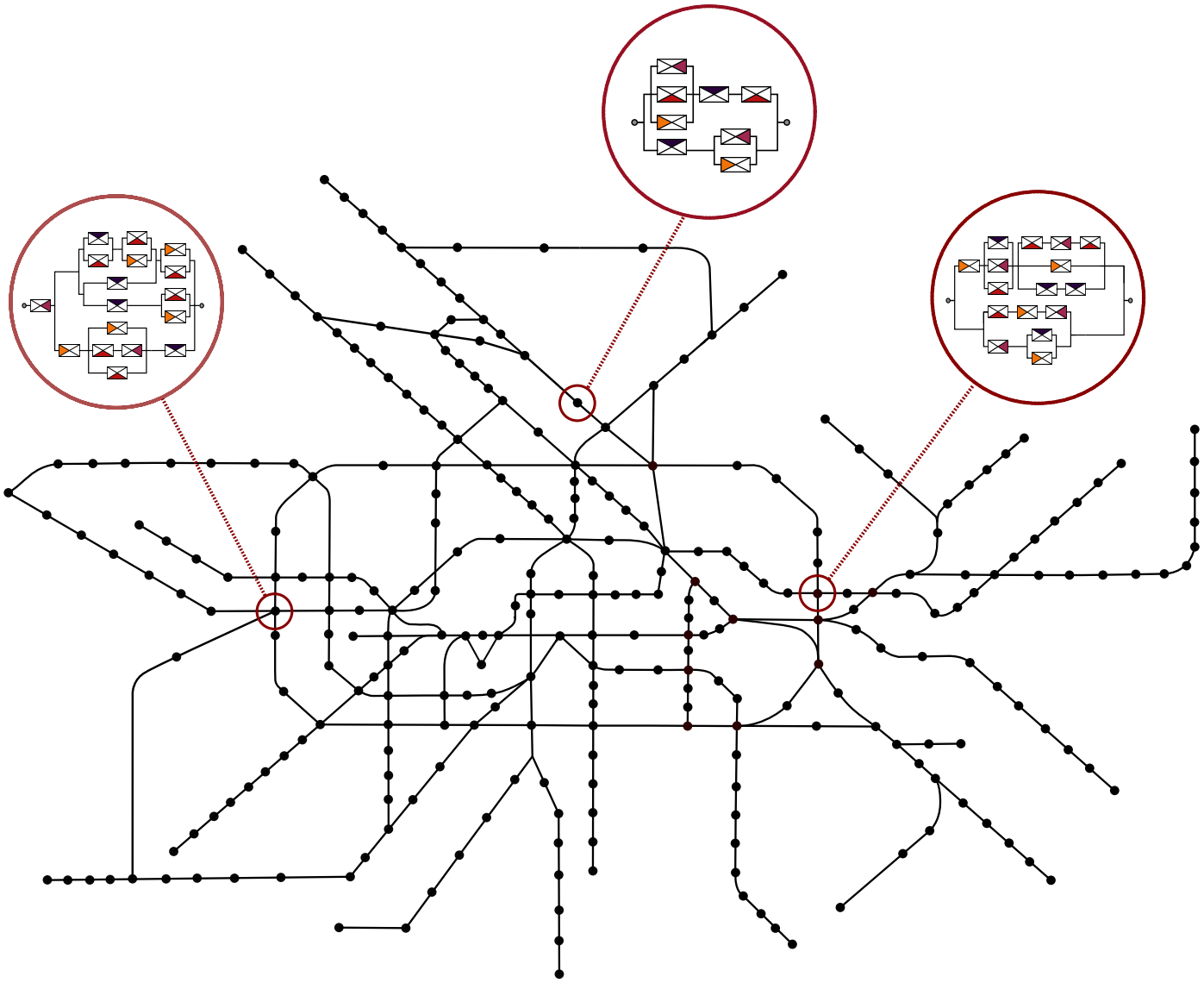

Figure 10: Topological network for the Berlin metro system.

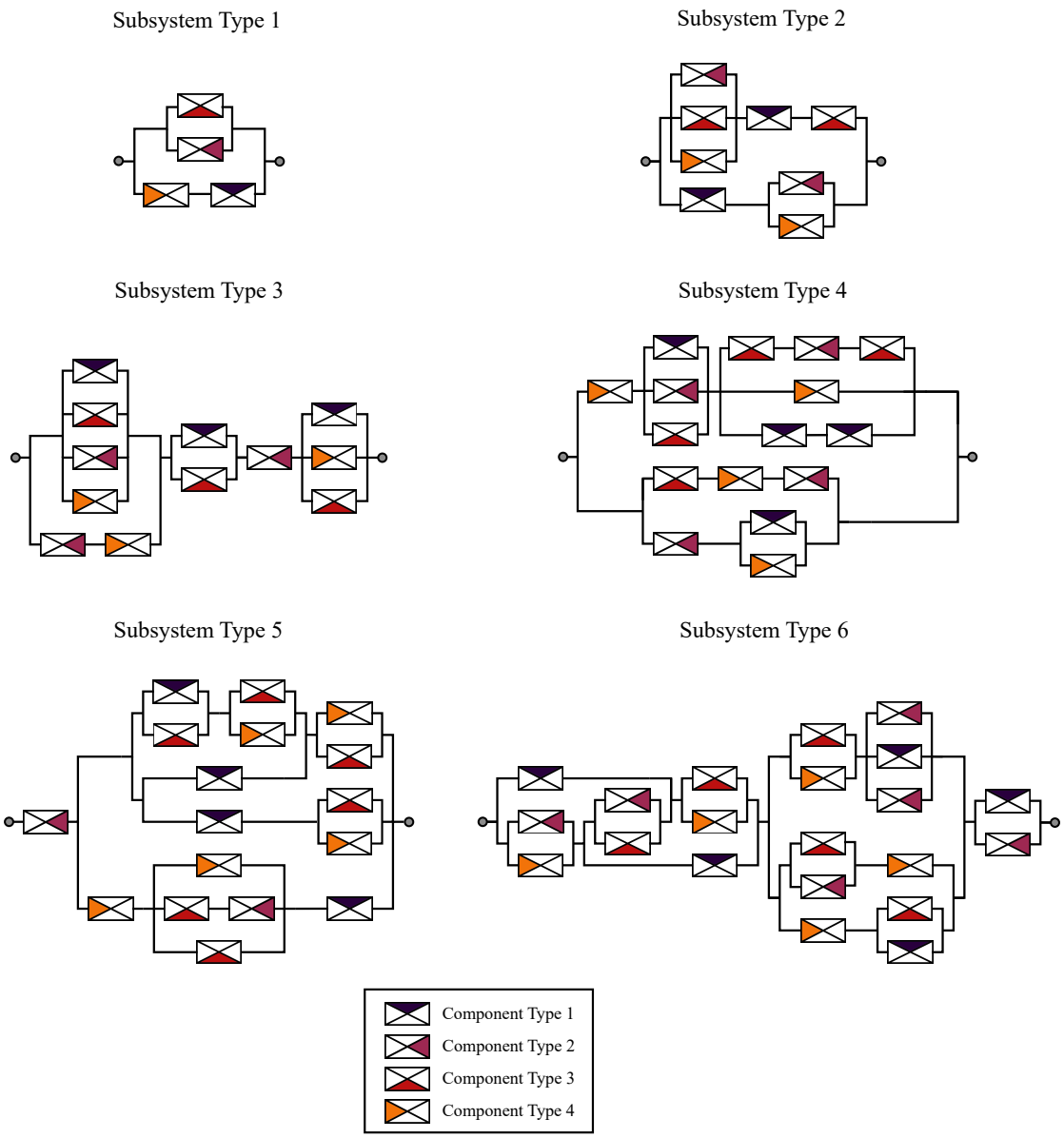

Figure 11: Representation of the $B = 6$ station types of the Berlin metro system.

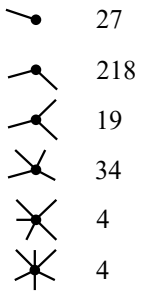

Figure 12: Number of individual metro stations per type.

the path length d_{uv} between stations, such as the algorithms of Floyd, Dijkstra's, or Bellman-Ford, is provided in [67] and [68].

The simulation procedure corresponds to that from the previous case study and the failure probability of a subsystem $\mathcal{S}_j$, i.e., metro station, in the time interval (t_h, t_{h+1}) is defined by Eq. (23). Unlike in the previous case study, a failed metro station is not entirely removed from the system, but remains in the set of metro stations; however, their node degree becomes 0, i.e., all existing connections to direct neighbors are removed. This assumption is essential, as the computation and interpretation of the system performance network efficiency depends on the number of nodes. The case study therefore relies on the fact that the number of nodes is constant.

If a subsystem $\mathcal{S}_j$ failed, its functionality is assumed to be immediately and fully recovered after a certain number of time steps r:

$$r = r_{\max} - 2 \cdot rec_j \quad \text{with} \quad rec_j < r_{\max}, \tag{28}$$

where rec_j is the recovery improvement specific to the station $\mathcal{S}_j$ and r_{max} is an upper bound for number of time-steps for recovery. After recovery, all previous connections to other metro stations are assumed to be restored, unless these are in a state of failure. As each time-step has a specific length of $\Delta t = (T/u)$, the duration of the recovery process is $r \cdot (T/u)$. Again, this recovery model corresponds to a one-step recovery profile and as mentioned before, various alternative characteristic profiles of recovery are possible as well. A repaired station and thus all components of the station are assumed to be in a as-new original condition after repair. This is an assumption for the sake of demonstration, and deviating states are possible. After recovery, the survival function of a metro station is time-zeroed, such that the resulting failure rate per simulation step $\lambda^{s_j}(t_h)$ evolves over time equivalent to that of a station in new condition.

7.2. Costs of Endowment Properties

The improvement of both endowment properties, "reliability improvement" and "recovery improvement", is inevitably associated with costs. Again, exponential relationships between total costs and improvements are assumed:

$$cost^{rel} = \sum_{i=1}^{2776} price^{rel}_{(rel_i;k_i)} \cdot 1.2^{(rel_i - 1)}, \tag{29}$$

where rel_i is the reliability improvement value of component i, k_i its type and $price^{rel}_{(rel_i;k_i)}$ an arbitrary common basic price. Accordingly an exponential relationship is assumed for the total cost associated with recovery improvement:

$$cost^{rec} = \sum_{j=1}^{306} price^{rec}_{(rec_j;b_j)} \cdot 1.2^{(rec_j - 1)}, \tag{30}$$

where rec_j is the recovery improvement value of station j, b_j its type and $price^{rec}_{(rec_j;b_j)}$ an arbitrary common basic price. The total cost $cost_{(A;z),(D;h)}$ of an endowment is the sum of these costs:

$$cost_{(A;z),(D;h)} = cost^{rel} + cost^{rec}. \tag{31}$$

In practice, it is crucial to include the economic aspects of failure and recovery processes in detail in the resilience assessment. Mitigating resilience losses through system improvements imposes direct costs on stakeholders, such as improving component properties. Note, however, that for a comprehensive analysis, it is important to also consider indirect costs to the affected population and businesses, when the performance of a key system declines, as stated in [28]. Further, it is reasonable to incorporate the subjective preferences of stakeholders into the resilience assessment, as suggested in [27]. These considerations have the potential to significantly influence the outcome of a resilience decision-making process. Therefore, they should be integrated into the proposed methodology in future work by including additional cost conditions and discount rates for the corresponding deterioration and recovery sequences.

7.3. Scenario

In order to apply the resilience decision-making method to the Berlin metro system illustrated in Fig. 10, the model parameter and simulation parameter values, shown in Tab. 4, are considered. The recovery improvement rec_j is explored over $rec_j \in \{1, \ldots, 10\}\ \forall j \in \{1, \ldots, 306\}$, but considered to be equal for each station, regardless of the type b_j. The reliability improvement rel_i again is explored over $rel_i \in \{1, \ldots, 10\}\ \forall i \in \{1, \ldots, 2776\}$ for $k_i \in \{1, \ldots, 4\}$.

In a pre-processing step, the survival signatures of all 306 metro stations are determined. As an example, Tab. 5 illustrates the non-trivial survival signature values, i.e., $\Phi(l_1, \ldots, l_4) \neq 0$ and $\Phi(l_1, \ldots, l_4) \neq 1$, of station type 2 of the metro system. Then, the set of all acceptable endowment configurations $R(Y)$, corresponding to a resilience value of at least $Res = 0.99$ over the considered time period, is determined according to Algorithm 4.3. Further, as any improvement of the system components and stations is associated with costs, the most cost-efficient acceptable endowment, denoted by the tuple $(\hat{A}, \hat{D})$, is determined.

In Fig. 13 the results of the grid search algorithm are illustrated. It shows the accepted endowments contained in $R(Y)$, i.e. all combinations that lead to a satisfying resilience of the metro system. It is clearly visible that type 1 components as well as the recovery improvement of the metro stations have the greatest influence and thus the highest importance for the metro system. Only endowments with a reliability improvement of at least $rel_i = 8$ for type 1 components and endowments with a recovery improvement for all metro stations of at least $rec_j = 8$ lead to a

Table 4: Parameter values for the resilience decision-making method on the metro system of Berlin.

Parameter	Scenario
Acceptance threshold α	0.99
Length of time step Δt	0.05
Number of time steps u	200
Maximum time T	10
Shape parameter gamma distribution α_i	$\alpha_i = 1.2$ for $k_i = 2$
	$\alpha_i = 2.6$ for $k_i = 4$
Maximum failure rate $\lambda_{i,\max}$	$\lambda_{i,\max} = 0.34$ for $k_i = 1$
	$\lambda_{i,\max} = 0.43$ for $k_i = 2$
	$\lambda_{i,\max} = 0.36$ for $k_i = 3$
	$\lambda_{i,\max} = 0.66$ for $k_i = 4$
Failure rate reduction $\Delta\lambda_i$	$\Delta\lambda_i = 0.03$ for $k_i = 1$
	$\Delta\lambda_i = 0.04$ for $k_i = 2$
	$\Delta\lambda_i = 0.034$ for $k_i = 3$
	$\Delta\lambda_i = 0.051$ for $k_i = 4$
Reliability improvement rel_i	$rel_i \in \{1, \ldots, 10\}$ for $k_i \in \{1, \ldots, 4\}$
Reliability improvement price $price^{rel}_{(rel_i;k_i)}$	$price^{rel}_{(rel_i;1)} = 100$€
	$price^{rel}_{(rel_i;2)} = 200$€
	$price^{rel}_{(rel_i;3)} = 200$€
	$price^{rel}_{(rel_i;4)} = 400$€
Maximum recovery time r_{max}	22
Recovery improvement rec_j	$rec_j \in \{1, \ldots, 10\}$
Recovery improvement price $price^{rec}_{(rec_j;b_i)}$	$price^{rec}_{(rec_j;1)} = 100$€
	$price^{rec}_{(rec_j;2)} = 200$€
	$price^{rec}_{(rec_j;3)} = 300$€
	$price^{rec}_{(rec_j;4)} = 400$€
	$price^{rec}_{(rec_j;5)} = 500$€
	$price^{rec}_{(rec_j;6)} = 600$€
Sample size N	500

Table 5: Non-trivial survival signature values of stations with $b_j = 2$ of the metro system, shown in Fig. 11.

l_1	l_2	l_3	l_4	$\Phi(l_1, \ldots, l_4)$
2	2	1	1	1/4
2	1	1	2	1/4
2	2	2	1	3/8
2	2	1	2	3/8
2	1	2	2	3/8
3	2	1	1	1/2
2	3	1	1	1/2
2	1	3	1	1/2
3	1	1	2	1/2
2	3	1	2	1/2
2	1	1	3	1/2
2	2	1	3	1/2
2	3	1	3	1/2
2	2	2	2	9/16
3	2	2	1	3/4
2	3	2	1	3/4
2	2	3	1	3/4
3	2	1	2	3/4
3	1	2	2	3/4
2	3	2	2	3/4
2	1	3	2	3/4
2	1	2	3	3/4
2	2	2	3	3/4
2	3	2	3	3/4
3	2	2	2	7/8
2	2	3	2	7/8

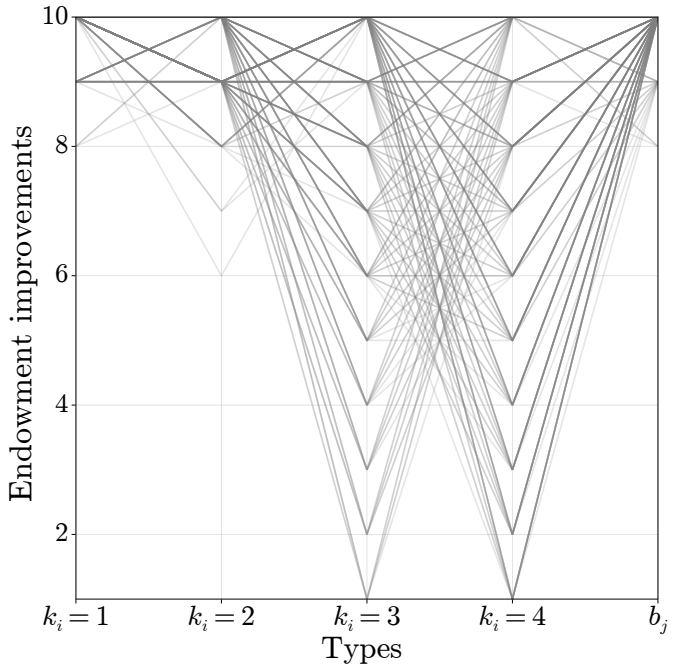

Figure 13: The set of all accepted endowments $R(Y)$ evaluated via the 5D grid search algorithm for the Berlin metro system with explored reliability improvement and recovery improvement values.

system resilience meeting the acceptance criterion. In addition, type 2 components are of considerable relevance. Here, only endowments with a reliability improvement of at least $rel_i = 6$ are acceptable. The reliability improvements of type 3 and 4 components, on the other hand, are of less significance. For both types of components, there are numerous acceptable configurations that include minimum reliability improvement values for one of these types.

These results again prove to be plausible, as in the previous case study, upon closer examination of the topological structures of the metro system and its subsystems. Several U-Bahn and S-Bahn lines start and end in long chains of directly interconnected type 2 stations, see Fig. 10. The resilience analysis of the Berlin metro system published in [20] revealed that especially an interruption of these chains has a major negative impact on the network efficiency and thus on the resilience of the metro system. Accordingly, the importance of type 2 stations is particularly high not only due to their multiplicity in the system, but due to their topological contribution in terms of connectivity as well. Consequently, components of this station type have a significant impact on the resilience of the overall system. An examination of the type 2 subsystem model, see Fig. 11, shows that type 1 components take on a predominant position. Once both type 1 components in this subsystem fail, the entire metro station fails. No other components of a single type can cause this in station type 2.

The significant influence of type 2 components can easily be explained by examining the type 3 and 5 station systems, see again Fig. 11. Of all stations, only here bottleneck positions exist, where the failure of a single component interrupts the functioning of the entire station. Both of these positions, in type

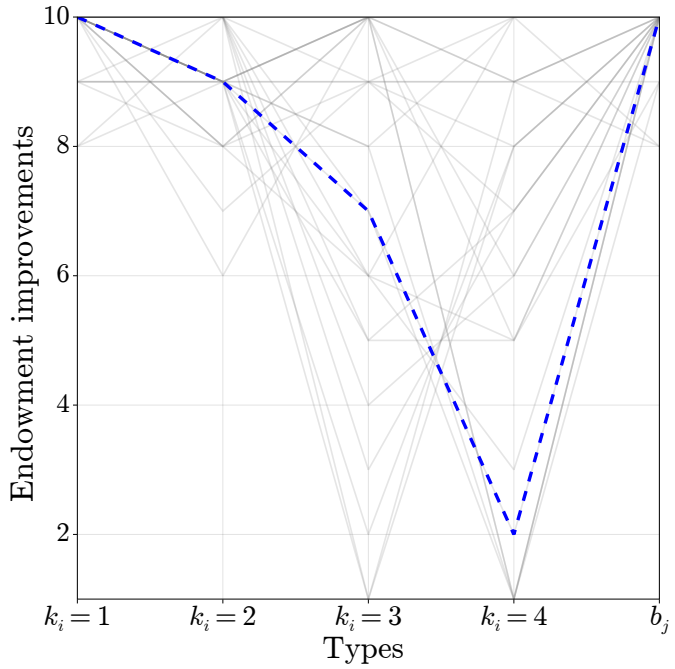

Figure 14: Dominant Pareto front endowments of the 5D grid search algorithm for the Berlin metro system with explored reliability improvement and recovery improvement values and the most cost-efficient endowment $(\hat{A}, \hat{D})$ is highlighted.

3 and type 5 stations, are occupied by type 2 components. Since both station types have three and five direct connections to other stations, they can be considered to be particularly interconnected and thus of high relevance to network efficiency and thus of high relevance to system resilience.

Type 3 and 4 components, on the other hand, do not occupy any particularly significant positions in the stations' systems. This explains their low influence. The enormous influence of the recovery improvement is intuitively explainable. As resilience is established via the integral of the actual system performance, each recovered metro station contributes directly and immediately to the network efficiency and thus to the resilience of the system. Therefore, improvement of this property results in an immediate and intuitive increase in resilience.

Assuming the arbitrary base prices in Tab. 4, the most cost-efficient acceptable endowment $(\hat{A}, \hat{D})$ results from a reliability improvement configuration of $rel_i = 10$ for $k_i = 1$, $rel_i = 9$ for $k_i = 2$, $rel_i = 7$ for $k_i = 3$, $rel_i = 2$ for $k_i = 4$ for components of type 1 to 4 and a maximum recovery improvement configuration of $rec_j = 10$ for $b_j \in \{1, 2, 3, 4\}$, i.e., all stations, regardless of their type. In Fig. 14, the corresponding configuration is highlighted. Due to the monotonicity of the input-output model and the assumed monotonically increasing endowment costs, only the endowment configurations on the dominant vertices of the Pareto front have to be examined for the identification of the most cost-efficient endowment. Therefore, only these endowment configurations are shown in Fig. 14. The resulting costs are given by Eq. (29, 30, 31) with $cost_{(\hat{A},\hat{D})} = 1\,700\,829€ + 361\,185€ = 2\,062\,014€$.

Due to the utilization of the grid search algorithm, the computational effort could be significantly reduced in this case study as well – only 0.159% of all potential endowment configurations had to be examined in order to assign a distinct state to each configuration in the search space as accepted or not accepted. By means of the novel approach, the metro system could be reduced from its entirety of 2776 individual components to 306 components on the top-level with respect to the resilience analysis, drastically reducing the computational effort. Nevertheless, all 2776 components and their influence were considered. As in the case study of the axial compressor, not only the most cost-efficient endowment configuration can be identified but also investigations on configurations that are below certain budget limits can be conducted.

Note that, in this case study, as well as in the previous ones, various complexity variations such as so-called cascading failures, see [69, 70, 71], are possible to implement due to the time-step-accurate simulation. In the case of infrastructure systems, e.g., the increasingly frequent natural disasters can thus be considered, that typically have an impact as local phenomena and affect stations that are geographically close to each other. It has already been shown in [20] that these can be taken into account in the resilience decision-making analysis of infrastructure systems.

8. Conclusion and Outlook

This paper addresses the challenge of efficient multidimensional decision-making for complex and substructured systems between resilience-influencing parameters. By merging an extension of the resilience framework proposed in [20] with the survival signature, an efficient and novel methodology is derived. The approach allows for direct comparison of the impact of heterogeneous controls on system resilience, such as failure prevention and recovery improvement arrangements, both during the design phase as well as during any phase in the life cycle of already existing complex systems.

Due to the time-step accurate simulation of the system performance on system level during the resilience analysis, complexity extensions such as cascading failures and other dependency structures can be considered without difficulties. The new methodology has a high numerical efficiency. The majority of the endowment properties examined affect the probability structure of the system components. The numerous changes in the probability structure caused by constantly changing endowment properties during the resilience analysis can be ideally covered with minimal effort due to the separation property of the survival signature.

The novel approach includes a substructuring approach for large, complex systems. This and the integration of the survival signature allow for the propagation of subsystem reliabilities through any number of system levels to the top-level and lead to a significant reduction of the computational load. This way, and with the extension of the adapted systemic risk measure, it is now possible to analyze systems with a large number of components in terms of their resilience.

Monetary restrictions can easily be included in the analysis. More precisely, not only the most cost-efficient, accepted endowment is identified, but subsets of the set of all accepted

endowments below defined price levels can be formed. Budget limits can thus be specifically taken into account in the decision-making process.

The methodology is applied to three entirely distinct systems: A functional model of a multistage high-speed axial compressor, an arbitrary system consisting of numerous subsystems and components and a comprehensive substructured model of the metro system of Berlin, proofing wide and general applicability. All results obtained are plausible with the corresponding assumed model parameters. Note, that the approach can be utilized to systems of any kind.

In the development of our proposed methodology, some simplifying assumptions were made that do not accurately reflect reality. However, the authors strongly believe that the presented approach can be considered as a meaningful core development that, for a reality-based application on highly multifactorial systems, such as cyber-human-physical systems, should be combined with future as well as existing developments to ensure an efficient and comprehensive resilience decision-making analysis taking into account all technical and monetary aspects of modern socities.

Future work will address the incorporation of various existing extensions of the concept of survival signature, such as accounting for uncertainty and propagating it toward imprecise system resilience and considering multiple state or continuous component functionality. Further, future work regarding multi-dimensional parameter spaces must deal with the limitations in computing time and storage capacity in order to enable application to even higher-dimensional problems. Namely, techniques such as advanced sampling methods, e.g. Subset Simulation, see [72], must be investigated to further reduce numerical effort.

Acknowledgment

Funded by the Deutsche Forschungsgemeinschaft (DFG, German Research Foundation) SFB 871/3 119193472 and SPP 2388 501624329.

References

[1] G. Punzo, A. Tewari, E. Butans, M. Vasile, A. Purvis, M. Mayfield, L. Varga, Engineering resilient complex systems: the necessary shift toward complexity science, IEEE Systems Journal 14 (3) (2020) 3865–3874.

[2] H. T. Tran, M. Balchanos, J. C. Domerçant, D. N. Mavris, A framework for the quantitative assessment of performance-based system resilience, Reliability Engineering & System Safety 158 (2017) 73–84. doi:10.1016/j.ress.2016.10.014.

[3] G. P. Cimellaro, A. M. Reinhorn, M. Bruneau, Framework for analytical quantification of disaster resilience, Engineering Structures 32 (11) (2010) 3639–3649. doi:10.1016/j.engstruct.2010.08.008.

[4] B. M. Ayyub, Practical resilience metrics for planning, design, and decision making, ASCE-ASME Journal of Risk and Uncertainty in Engineering Systems, Part A: Civil Engineering 1 (3) (2015) 04015008. doi:10.1061/ajrua6.0000826.

[5] Y. Fang, N. Pedroni, E. Zio, Optimization of Cascade-Resilient Electrical Infrastructures and its Validation by Power Flow Modeling, Risk Analysis 35 (4) (2015) 594–607. doi:10.1111/risa.12396.

[6] G. P. Cimellaro, Urban resilience for emergency response and recovery, Fundamental Concepts and Applications (2016).

[7] A. Sharifi, Urban resilience assessment: Mapping knowledge structure and trends, Sustainability 12 (15) (2020) 5918.

[8] J. Bergström, R. Van Winsen, E. Henriqson, On the rationale of resilience in the domain of safety: A literature review, Reliability Engineering and System Safety 141 (2015) 131–141. doi:10.1016/j.ress.2015.03.008.

[9] R. Patriarca, J. Bergström, G. Di Gravio, F. Costantino, Resilience engineering: Current status of the research and future challenges, Safety Science 102 (2018) 79–100. doi:10.1016/j.ssci.2017.10.005.

[10] C. S. Holling, Resilience and Stability of Ecological Systems, Annu.Rev.Ecol.Syst. 4 (1973) 1–23. arXiv:arXiv:1011.1669v3, doi:10.1146/annurev.es.04.110173.000245.

[11] J. Fiksel, Designing Resilient, Sustainable Systems, Environmental Science and Technology 37 (23) (2003) 5330–5339. doi:10.1021/es0344819.

[12] R. G. Little, Toward more robust infrastructure: Observations on improving the resilience and reliability of critical systems, Proceedings of the 36th Annual Hawaii International Conference on System Sciences, HICSS 2003 (2003). doi:10.1109/HICSS.2003.1173880.

[13] E. Hollnagel, D. E. Woods, N. Levensen, Resilience Engineering: Concepts and Precepts, Aldershot, UK: Ashgate Publishing, 2006.

[14] M. Bruneau, A. Reinhorn, Exploring the concept of seismic resilience for acute care facilities, Earthquake Spectra 23 (1) (2007) 41–62. doi:10.1193/1.2431396.

[15] B. D. Youn, C. Hu, P. Wang, Resilience-Driven System Design of Complex Engineered Systems, Journal of Mechanical Design 133 (10) (2011) 101011. doi:10.1115/1.4004981.

[16] B. M. Ayyub, Systems resilience for multihazard environments: Definition, metrics, and valuation for decision making, Risk Analysis 34 (2) (2014) 340–355. doi:10.1111/risa.12093.

[17] Presidential Policy Directive (PPD), Critical infrastructure security and resilience, (accessed Nov. 9, 2018) (2013).
URL https://obamawhitehouse.archives.gov/the-press-office/2013/02/12/presidential-policy-directive-critical-infrastructure-security-

[18] S. Gilbert, B. M. Ayyub, Models for the Economics of Resilience, ASCE-ASME Journal of Risk and Uncertainty in Engineering Systems, Part A: Civil Engineering 2 (2016).

[19] Y. Fang, G. Sansavini, Optimizing power system investments and resilience against attacks, Reliability Engineering and System Safety 159 (2017) 161–173. doi:10.1016/j.ress.2016.10.028.
URL http://dx.doi.org/10.1016/j.ress.2016.10.028

[20] J. Salomon, M. Broggi, S. Kruse, S. Weber, M. Beer, Resilience decision-making for complex systems, ASCE-ASME J Risk and Uncert in Engrg Sys Part B Mech Engrg 6 (2) (2020).

[21] M. Ouyang, L. Dueñas-Osorio, X. Min, A three-stage resilience analysis framework for urban infrastructure systems, Structural Safety 36-37 (2012) 23–31. doi:10.1016/j.strusafe.2011.12.004.

[22] Z. Feinstein, B. Rudloff, S. Weber, Measures of Systemic Risk, SIAM Journal on Financial Mathematics 8 (1) (2017) 672 –708.

[23] R. R. Singh, M. Bruneau, A. Stavridis, K. Sett, Resilience deficit index for quantification of resilience, Resilient Cities and Structures 1 (2) (2022) 1–9. doi:https://doi.org/10.1016/j.rcns.2022.06.001.

[24] A. Alipour, B. Shafei, An overarching framework to assess the life-time resilience of deteriorating transportation networks in seismic-prone regions, Resilient Cities and Structures 1 (2) (2022) 87–96. doi:https://doi.org/10.1016/j.rcns.2022.07.002.

[25] L. Capacci, F. Biondini, D. M. Frangopol, Resilience of aging structures and infrastructure systems with emphasis on seismic resilience of bridges and road networks: Review, Resilient Cities and Structures 1 (2) (2022) 23–41. doi:https://doi.org/10.1016/j.rcns.2022.05.001.

[26] S. Duan, B. M. Ayyub, Assessment methods of network resilience for cyber-human-physical systems, ASCE-ASME Journal of Risk and Uncertainty in Engineering Systems, Part A: Civil Engineering 6 (1) (2020) 03119001.

[27] R. Emanuel, B. Ayyub, Assessing resilience model responsiveness in the context of stakeholder preferences in decision support systems, ASCE-ASME Journal of Risk and Uncertainty in Engineering Systems, Part A: Civil Engineering 5 (2) (2019) 04019005.

[28] Y. Saadat, B. M. Ayyub, Y. Zhang, D. Zhang, H. Huang, Resilience-based strategies for topology enhancement and recovery of metrorail transit networks, ASCE-ASME Journal of Risk and Uncertainty in Engineering Systems, Part A: Civil Engineering 6 (2) (2020) 04020017. doi:10.

1061/AJRUA6.0001057.
[29] Y. Zhang, B. M. Ayyub, J. F. Fung, Projections of corrosion and deterioration of infrastructure in united states coasts under a changing climate, Resilient Cities and Structures 1 (1) (2022) 98–109. doi:https://doi.org/10.1016/j.rcns.2022.04.004.
[30] C. B. Nielsen, P. G. Larsen, J. Fitzgerald, J. Woodcock, J. Peleska, Systems of systems engineering: basic concepts, model-based techniques, and research directions, ACM Computing Surveys (CSUR) 48 (2) (2015) 1–41.
[31] M. Jamshidi, Systems of systems engineering: principles and applications, CRC press, 2017.
[32] M. Batty, Complexity in city systems: Understanding, evolution, and design, in: A planner's encounter with complexity, Routledge, 2016, pp. 99–122.
[33] K. Kolowrocki, Reliability of large and complex systems, Elsevier, 2014.
[34] S. Negi, S. Singh, Reliability analysis of non-repairable complex system with weighted subsystems connected in series, Applied Mathematics and Computation 262 (2015) 79–89.
[35] F. P. Coolen, T. Coolen-Maturi, Generalizing the signature to systems with multiple types of components, in: Complex Systems and Dependability, Springer, 2013, pp. 115–130. doi:10.1007/978-3-642-30662-4_8.
[36] F. P. Coolen, T. Coolen-Maturi, The structure function for system reliability as predictive (imprecise) probability, Reliability Engineering & System Safety 154 (2016) 180–187. doi:10.1016/j.ress.2016.06.008.
[37] E. Patelli, G. Feng, F. P. Coolen, T. Coolen-Maturi, Simulation methods for system reliability using the survival signature, Reliability Engineering & System Safety 167 (2017) 327–337.
[38] G. Feng, H. George-Williams, E. Patelli, F. Coolen, M. Beer, An efficient reliability analysis on complex non-repairable systems with common-cause failures, in: Safety and Reliability–Safe Societies in a Changing World, CRC Press, 2018, pp. 2531–2537.
[39] H. George-Williams, G. Feng, F. P. Coolen, M. Beer, E. Patelli, Extending the survival signature paradigm to complex systems with non-repairable dependent failures, Proceedings of the Institution of Mechanical Engineers, part O: journal of risk and reliability 233 (4) (2019) 505–519.
[40] J. Behrensdorf, T.-E. Regenhardt, M. Broggi, M. Beer, Numerically efficient computation of the survival signature for the reliability analysis of large networks, Reliability Engineering & System Safety 216 (2021) 107935.
[41] J. Salomon, N. Winnewisser, P. Wei, M. Broggi, M. Beer, Efficient reliability analysis of complex systems in consideration of imprecision, Reliability Engineering & System Safety 216 (2021) 107972.
[42] S. Hosseini, K. Barker, J. E. Ramirez-Marquez, A review of definitions and measures of system resilience, Reliability Engineering & System Safety 145 (2016) 47–61. doi:10.1016/j.ress.2015.08.006.
[43] W. Sun, P. Bocchini, B. D. Davison, Resilience metrics and measurement methods for transportation infrastructure: the state of the art, Sustainable and Resilient Infrastructure 5 (3) (2020) 168–199.
[44] D. Henry, J. E. Ramirez-Marquez, Generic metrics and quantitative approaches for system resilience as a function of time, Reliability Engineering and System Safety 99 (2012) 114–122. doi:10.1016/j.ress.2011.09.002.
[45] M. Bruneau, S. E. Chang, R. T. Eguchi, G. C. Lee, T. D. O'Rourke, A. M. Reinhorn, M. Shinozuka, K. Tierney, W. A. Wallace, D. Von Winterfeldt, A framework to quantitatively assess and enhance the seismic resilience of communities, Earthquake spectra 19 (4) (2003) 733–752.
[46] C. W. Zobel, Representing perceived tradeoffs in defining disaster resilience, Decision Support Systems 50 (2) (2011) 394–403.
[47] T. M. Adams, K. R. Bekkem, E. J. Toledo-Durán, Freight resilience measures, Journal of Transportation Engineering 138 (11) (2012) 1403–1409.
[48] N. Sahebjamnia, S. A. Torabi, S. A. Mansouri, Integrated business continuity and disaster recovery planning: Towards organizational resilience, European Journal of Operational Research 242 (1) (2015) 261–273.
[49] S. Weber, K. Weske, The joint impact of bankruptcy costs, fire sales and cross-holdings on systemic risk in financial networks, Probability, Uncertainty and Quantitative Risk 2 (1) (2017). doi:10.1186/s41546-017-0020-9.
URL https://doi.org/10.1186/s41546-017-0020-9
[50] G. Feng, E. Patelli, M. Beer, F. P. Coolen, Imprecise system reliability and component importance based on survival signature, Reliability Engineering & System Safety 150 (2016) 116–125. doi:10.1016/j.ress.2016.01.019.
[51] S. Eryilmaz, A. Tuncel, Generalizing the survival signature to unrepairable homogeneous multi-state systems, Naval Research Logistics (NRL) 63 (8) (2016) 593–599.
[52] Y. Liu, Y. Shi, X. Bai, B. Liu, Stress–strength reliability analysis of multi-state system based on generalized survival signature, Journal of Computational and Applied Mathematics 342 (2018) 274–291.
[53] H. Yi, L. Cui, N. Balakrishnan, Computation of survival signatures for multi-state consecutive-k systems, Reliability Engineering & System Safety 208 (2021) 107429.
[54] J. Qin, F. P. Coolen, Survival signature for reliability evaluation of a multi-state system with multi-state components, Reliability Engineering & System Safety 218 (2022) 108129.
[55] F. P. Coolen, T. Coolen-Maturi, A. H. Al-Nefaiee, Nonparametric predictive inference for system reliability using the survival signature, Proceedings of the Institution of Mechanical Engineers, Part O: Journal of Risk and Reliability 228 (5) (2014) 437–448.
[56] J. Behrensdorf, J. Salomon, N. Winnewisser, ResilienceDecisionMaking.jl (2022). doi:10.5281/zenodo.7034998.
[57] S. Miro, T. Willeke, M. Broggi, J. Seume, M. Beer, Reliability analysis of an axial compressor based on one-dimensional flow modeling and survival signature, ASCE-ASME Journal of Risk and Uncertainty in Engineering Systems, Part B: Mechanical Engineering 5 (3) (2019) 031003. doi:10.1115/1.4043150.
[58] M. Braun, J. R. Seume, Forward sweep in a four-stage high-speed axial compressor, in: ASME Turbo 2006: Power for Land, Sea, and Air, Vol. Volume 6: Turbomachinery, Parts A and B, American Society of Mechanical Engineers, 2008, pp. 141–152. doi:10.1115/GT2006-90218.
[59] B. Hellmich, J. Seume, Causes of acoustic resonance in a high-speed axial compressor, ASME. J. Turbomach. 130 (3) (2008) 031003. doi:10.1115/1.2775487.
[60] J. Siemann, I. Krenz, J. R. Seume, Experimental investigation of aspiration in a multi-stage high-speed axial-compressor, in: ASME Turbo Expo 2016: Power for Land, Sea, and Air, Vol. Volume 2A: Turbomachinery, American Society of Mechanical Engineers, 2016, p. V02AT37A010. doi:10.1115/GT2016-56440.
[61] A. Mettas, Reliability allocation and optimization for complex systems, Reliability and Maintainability Symposium, 2000. Proceedings. Annual (2000) 216–221doi:10.1109/RAMS.2000.816310.
[62] Berliner Verkehrsbetriebe, Lagebericht und Jahresabschluss 2017, (accessed Oct. 5, 2018) (2018).
URL http://unternehmen.bvg.de/index.php?section=downloads{&}download=3128
[63] S-Bahn Berlin, https://sbahn.berlin/das-unternehmen/unternehmensprofil/s-bahn-berlin-auf-einen-blick/, (accessed Oct. 5, 2018) (2018). [link].
URL https://sbahn.berlin/das-unternehmen/unternehmensprofil/s-bahn-berlin-auf-einen-blick/
[64] K. M. Zuev, S. Wu, J. L. Beck, General network reliability problem and its efficient solution by Subset Simulation, Probabilistic Engineering Mechanics 40 (2015) 25–35. doi:10.1016/j.probengmech.2015.02.002.
URL http://dx.doi.org/10.1016/j.probengmech.2015.02.002
[65] J. Zhang, M. Zhao, H. Liu, X. Xu, Networked characteristics of the urban rail transit networks, Physica A: Statistical Mechanics and its Applications 392 (6) (2013) 1538–1546.
[66] V. Latora, M. Marchiori, Efficient behavior of small-world networks, Physical Review Letters 87 (19) (2001) 198701–1–198701–4. arXiv:0101396, doi:10.1103/PhysRevLett.87.198701.
[67] S. E. Dreyfus, An Appraisal of Some Shortest-Path Algorithms, Operations Research 17 (3) (1969) 395–412.
[68] F. B. Zhan, C. E. Noon, Shortest Path Algorithms: An Evaluation Using Real Road Networks, Transportation Science 32 (1998) 65–73. doi:10.1287/trsc.32.1.65.
[69] P. Crucitti, V. Latora, M. Marchiori, Model for cascading failures in complex networks, Physical Review E - Statistical Physics, Plasmas, Fluids, and Related Interdisciplinary Topics 69 (4) (2004) 4. arXiv:0309141, doi:10.1103/PhysRevE.69.045104.
[70] L. Dueñas-Osorio, S. M. Vemuru, Cascading failures in complex infrastructure systems, Structural Safety 31 (2) (2009) 157–167. doi:10.1016/j.strusafe.2008.06.007.

URL http://dx.doi.org/10.1016/j.strusafe.2008.06.007
[71] S. V. Buldyrev, R. Parshani, G. Paul, H. E. Stanley, S. Havlin, Catastrophic cascade of failures in interdependent networks, Nature 464 (7291) (2010) 1025–1028. doi:10.1038/nature08932.
URL http://dx.doi.org/10.1038/nature08932
[72] S.-K. Au, Y. Wang, Engineering risk assessment with subset simulation, John Wiley & Sons, 2014.